Received: 9 March 2016 | Accepted: 9 May 2017
DOI: 10.1002/hyp.11224

WILEY

RESEARCH ARTICLE

The importance of aspect for modelling the hydrological response in a glacier catchment in Central Asia

Hongkai Gao[1,2,3] | **Yongjian Ding**[2] | **Qiudong Zhao**[2] | **Markus Hrachowitz**[4] | **Hubert H.G. Savenije**[4]

[1] Guangdong Engineering Technology Research Center of Water Security Regulation and Control for Southern China, Sun Yat-sen University, Guangzhou 510275, China

[2] State Key Laboratory of Cryosheric Sciences, Cold and Arid Regions Environmental and Engineering Research Institute, Chinese Academy of Sciences, Lanzhou, China

[3] Julie Ann Wrigley Global Institute of Sustainability, Arizona State University, Tempe, AZ 85287, USA

[4] Water Resources Section, Delft University of Technology, Delft, Netherlands

Correspondence
Hongkai Gao, Guangdong Engineering Technology Research Center of Water Security Regulation and Control for Southern China, Sun Yat-sen University, Guangzhou 510275, China.
Email: gaohongkai2005@126.com

Funding information
National Basic Research Program of China, Grant/Award Number: 2013CBA01808-A; State Key Laboratory of Cryospheric Sciences, Cold and Arid Regions Environment and Engineering Research Institute, Chinese Academy Sciences, Grant/Award Number: SKLCS-OP-2016-04; Natural Science Foundation of China, Grant/Award Number: 41130638, 41271090, 41471001, 51479216 and 91547202

Abstract

Understanding how explicit consideration of topographic information influences hydrological model performance and upscaling in glacier dominated catchments remains underexplored. In this study, the Urumqi glacier no. 1 catchment in northwest China, with 52% of the area covered by glaciers, was selected as study site. A conceptual glacier-hydrological model was developed and tested to systematically, simultaneously, and robustly reproduce the hydrograph, separate the discharge into contributions from glacier and nonglacier parts of the catchment, and establish estimates of the annual glacier mass balance, the annual equilibrium line altitude, and the daily catchment snow water equivalent. This was done by extending and adapting a recently proposed landscape-based semidistributed conceptual hydrological model (FLEX-Topo) to represent glacier and snowmelt processes. The adapted model, $FLEX^{G}$, allows to explicitly account for the influence of topography, that is, elevation and aspect, on the distribution of temperature and precipitation and thus on melt dynamics. It is shown that the model can not only reproduce long-term runoff observations but also variations in glacier and snow cover. Furthermore, $FLEX^{G}$ was successfully transferred and up-scaled to a larger catchment exclusively by adjusting the areal proportions of elevation and aspect without the need for further calibration. This underlines the value of topographic information to meaningfully represent the dominant hydrological processes in the region and is further exacerbated by comparing the model to a model formulation that does not account for differences in aspect ($FLEX^{G,nA}$) and which, in spite of satisfactorily reproducing the observed hydrograph, does not capture the influence of spatial variability of snow and ice, which as a consequence reduces model transferability. This highlights the importance of accounting for topography and landscape heterogeneity in conceptual hydrological models in mountainous and snow-, and glacier-dominated regions.

KEYWORDS

FLEX-Topo, glacier melt, temperature-index model, topography, Urumqi no.1 glacier

1 | INTRODUCTION

The mountainous region in Central Asia as the water tower for surrounding regions (Immerzeel, van Beek, & Bierkens, 2010) provides precious water resources for millions of residents living in downstream regions (Ding, Liu, Li, & Shangguan, 2006), for the agricultural and industrial development (Li, Cheng, et al., 2013; Singh & Singh, 2001) and ecosystems conservation (Zhao & Cheng, 2002). On the one hand, glacier- and snow melt-derived water is one of the most important water resources in the arid northwest of China (Cheng et al., 2014; Duethmann, Menz, Jiang, & Vorogushyn, 2016; Qin & Ding, 2010; Shi, Huang, & Yao, 2000; Yao, Pu, Lu, Wang, & Yu, 2007), and other regions in Central Asia and the Himalayas (Bhutiyani, Kale, & Pawar, 2008; Immerzeel et al., 2010; Raina, Srivastava, Singh, & Sangewar, 2008; Sorg, Bolch, Stoffel, Solomina, & Beniston, 2012; Unger-Shayesteh et al., 2013). On the other hand, changes to glaciers and the amount and timing of snow cover are highly sensitive to climate change (Oerlemans & Fortuin, 1992; Thayyen & Gergan, 2010; Thayyen, Gergan, & Dobhal, 2005; Yao et al., 2012), which may threaten the downstream water security (Berghuijs, Woods, & Hrachowitz, 2014; Immerzeel et al., 2010) and increase the risks of natural hazards (Liu et al., 2014; Moore et al., 2009). To systematically understand both, the water balance and hydrological processes in this region, it is crucial to integrate observational data and our knowledge on hydrological processes of this region into robust hydrological models. The specific heterogeneities in these mountainous environment and the complex landscapes underline the need for tailor-made hydrological models with the skill to simultaneously account for the effect of these landscape heterogeneities on glacier and snowpack variation, from both scientific and practical perspective.

Glacier and snow melt models can be categorized into two classes. On the one hand, there are energy balance based models (Blöschl, Kirnbauer, & Gutknecht, 1991; Gelfan, Pomeroy, & Kuchment, 2004; Hock, 2005; Ohmura et al., 1994; Pomeroy et al., 2007) that require detailed and rarely available observations of surface energy fluxes to estimate snow and ice accumulation and melt. On the other hand, temperature-index models (e.g., Braithwaite & Olesen, 1989; Hock, 2003; Schaefli, Hingray, Niggli, & Musy, 2005; Zhang, Liu, & Ding, 2006) provide a simple yet valuable alternative, only requiring more widely available temperature data, although station-based temperature data are also scarce in this region and remote sensing data requires careful downscaling before being employed. In spite of its simple and conceptual nature, the temperature-index method has in the past been shown to be a useful integrated indicator for overall catchment energy budgets (Hock, 2003).

In previous research, relatively simple formulations of glacier melt have been coupled with hydrological models, such as HBV (Hydrologiska Byråns Vattenbalansavdelning, e.g., Konz & Seibert, 2010), and GSM-SOCONT (Glacier and SnowMelt-SOil CONTribution Model, Schaefli et al., 2005). A glacio-hydrological model, coupled with distributed temperature-index model, surface runoff, glacial storage and transport, subglacial drainage and flow in a subsurface aquifer, was developed and successfully tested by Flowers and Clarke (2002). Other glacier processes and evolution such as retreat and area shrinkage were also suggested for glacio-hydrological models (e.g., Huss, Jouvet, Farinotti, & Bauder, 2010; Immerzeel, van Beek, Konz, Shrestha, & Bierkens, 2012; Stahl, Moore, Shea, Hutchinson, & Cannon, 2008) and are important to predict glacio-hydrological variation under climate change. To calibrate and validate models, in situ observation and remote sensing products are increasingly acknowledged as valuable auxiliary information sources for glacier and snow hydrology simulation (Konz & Seibert, 2010; Parajka & Blöschl, 2008).

In Central Asia, the extremely inaccessible environment is one of the main reasons for the lack of long-term glacier, snow, and hydrometeorological observations. This causes a bottle neck for the development, implementation and rigorous testing of robust models, although a few glacio-hydrological models were successfully implemented in the poorly gauged glacier catchments of the Himalayas (Fujita & Sakai, 2014; Fujita et al., 2006), such as the TAC^{D} model (Konz, Uhlenbrook, Braun, Shrestha, & Demuth, 2007; Uhlenbrook, Roser, & Tilch, 2004) or SNOWMOD (Singh, Haritashya, & Kumar, 2008). Some published research applied snow and glacier data together with long-term variations of discharge for modelling macroscale estimates of hydrological fluxes in Northwest China (Duethmann et al., 2015; He, Tian, Gupta, Hu, & Hu, 2014; Zhao et al., 2013) and Central Asia in general (Duethmann, Peters, Blume, Vorogushyn, & Güntner, 2014; Sorg, Huss, Rohrer, & Stoffel, 2014). However, systematically testing and evaluating models against long-term observations at high spatio-temporal resolutions of meteorological, hydrologial, and snow- and glacier-related variables is, given the scarcity of data, still not well explored, in particularily for small catchments.

In mountainous and glacier-covered catchments, topography directly and considerably affects various meteorological factors, for example, precipitation and temperature (Barry, 1992), which have considerable impact on hydrological processes. Aspect as an essential topographic factor is a dominant control on direct solar radiation and wind exposure and thus on snow and ice accumulation and ablation (Anderton, White, & Alvera, 2004; Biederman et al., 2014; Fujihara et al., 2017; Garvelmann, Pohl, & Weiler, 2015; Hock, 1999; Pohl, Garvelmann, Wawerla, & Weiler, 2014). In hydrological models, aspect has previously been considered not only in energy balance (Blöschl et al., 1991; Pomeroy et al., 2007) but also in temperature-index models (Dunn & Colohan, 1999; Hock, 1999; Seibert, 1997). Yet the importance of aspect for a meaningful representation of hydrological processes on the catchment scale and thus for spatial model transferability in snow- and glacier-dominated catchments is still not well explored. Model transferability is closely linked not only to model upscaling but also to predictions in ungauged basins (Hrachowitz et al., 2013), and it is a potentially strong test to assess a model's skill to adequately reproduce observed system dynamic by a suitable representation of dominant processes.

Furthermore, a hydrological model is a tool to systematically understand hydrological behaviour (Clark, Kavetski, & Fenicia, 2011; Fenicia, Savenije, Matgen, & Pfister, 2008). However, lack of data to test and evaluate model results, in particular the dynamics of system states and internal fluxes, remains an unresolved challenge in hydrological model development (Savenije & Hrachowitz, 2017). In addition, the absence of complete process understanding ("all models are simplifications"; Gupta, Wagener, & Liu, 2008) together with disinformative data ("a form of knowledge or *epistemic* error"; Beven & Westerberg, 2011) typically results in considerable model equifinality and thus uncertainties (Beven & Binley, 1992), which is in particular true for difficult to observe subsurface processes. In contrast to subsurface fluxes, spatial–temporal patterns of modelled glacier and snow variation can be evaluated by readily available and remotely sensed observations. In this case, glacier and snow data, as important complementary information, provide a good opportunity to evaluate modelled internal system dynamics in addition to a model's skill to reproduce the hydrograph. Such a focus on a wider range of system dynamics by making efficient use of available hard and soft information (e.g., Seibert & McDonnell, 2002; Hrachowitz et al., 2014) will increase the confidence in model results as a more rigorous model testing (e.g., Andréassian et al., 2012; Semenova & Beven, 2015).

In this study, we therefore extend and adapt a recently proposed landscape-based, semidistributed hydrological model, FLEX-Topo (Euser, Hrachowitz, Winsemius, & Savenije, 2015; Gao, Hrachowitz, Fenicia, et al., 2014; Gharari, Hrachowitz, Fenicia, et al., 2014; Savenije, 2010), to a glacier catchment in Central Asia. In particular we are going to test whether (a) a semidistributed conceptual model, with a parsimonious, topography guided formulation of a temperature-index based routine to simulate snow and ice melt, can simultaneously reproduce observed stream flow, and glacier and snowpack variations in the study catchment; (b) accounting for topographic information, that is, aspect, will increase the model's skill to reproduce observed hydrographs, as well as snow and glacier variations; and (c) explicitly incorporating aspect in the model formulation can improve the model's ability to be upscaled and spatially transferred.

2 | STUDY SITE AND DATA

2.1 | Study site

The Urumqi glacier no. 1 catchment is located in the headwaters of the Urumqi River, in the Xinjiang Uyghur Autonomous Region in northwest China (43°50′N, 86°49′E; Figure 1). Glacier no. 1 is a valley glacier with two branches, that is, east and west (Shi et al., 2000; Ye et al., 2005). The digital elevation model of the glacier no.1 in 90-m spatial resolution was obtained from geodetic survey in 2001 (Lanzhou Iinstitute of Glaciology and Geocryology, 2001). The two branches of the glacier cover a total area of about 1.84 km^2 and are both roughly 2.2-km long, being located at elevations between about 3,740 and 4,490 m a.s.l. The average ice thickness measured by radar in 2003 is about 50 m (Sun et al., 2003). Figure 1 shows that the aspect of glacier is mostly facing north and partly facing east/west.

The glacier observation program at the Tianshan glacier station started in 1959 (Xie & Ge, 1965) and continued up to the present day. Field observations include yearly glacier mass balance (GMB) measurements, as well as daily meteorological and hydrological data collection. The glacier accumulation and ablation is observed by the stake method and additional snow pits (Ye et al., 2005). The DXG (Da Xi Gou) is a meteorological station located in the catchment. Runoff is observed by two runoff gauging stations. The no. 1 (Urumqi glacier no. 1) runoff gauge station with a contributing drainage area of 3.3 km^2 has been set up 200-m downstream of the glacier terminus at 3,689 m a.s.l, with 52% of the area covered by glacier. Another gauge station, the ZK (Zong Kong), is located further downstream, controlling an area of 28.9km^2, with 19.4% covered by glaciers. The land cover in the nonglacier area is mainly bare soil/rock with sparse grass and seasonally covered by snow (Li, Wang, Zhang, Wang, & Li, 2010).

2.2 | Glacier descriptors

GMB and equilibrium line altitude (ELA) are two essential indicators to quantify the glacier change with climate change (Cuffey & Paterson, 2010). From monthly stake readings the mass balance at the observation point in that year can be estimated (Dong, Qin, Ren, Li, & Li, 2012; Ye et al., 2005). Contributions from several accumulation and ablation processes determine the GMB at a point:

$$\frac{dS_g}{dt} = P + A_a + A_w - Q_g - E_g, \tag{1}$$

where P [L/T] is precipitation, A_a [L/T] represents avalanches and A_w [L/T] represents wind deposition, Q_g [L/T] is discharge from the glacier, and E_g [L/T] is the sublimation rate. For long-term estimates of the GMB for the entire glacier $\frac{dS_g}{dt} = P - Q_g$ provides a robust approximation (Cuffey & Paterson, 2010) and was therefore here used to quantify the modelled GMB in this study. The ELA is the altitude at which ice

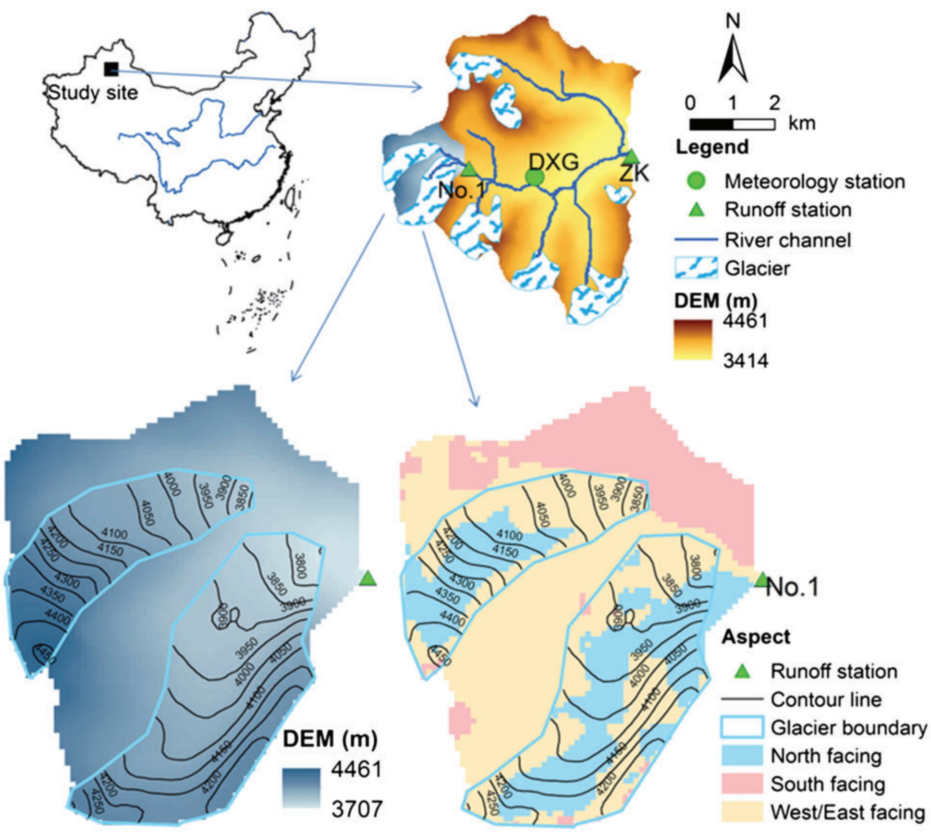

FIGURE 1 Locations of the glacier no. 1 (upper left), the Digital Elevation Model (DEM) and glaciers cover of the Zong Kong (ZK) catchment, the detailed DEM and contour lines of the nested glacier no. 1 catchment, and the aspects of the glacier no.1 catchment. DXG = Da Xi Gou

TABLE 1 Observed variables, the periods of observation, and the time step of data

Data	Period of observation	Time step
Discharge in No. 1	1985–1998, 2001–2004	Daily
Discharge in ZK	1985–1995, 1997–2004	Daily
Temperature	1959–2006	Daily
Precipitation	1959–2006	Daily
Snow water equivalent	March 1987–February 1988	Daily
GMB of glacier no. 1	1959–2006, (1967–1979 reconstructed)	Annual
ELA of glacier no. 1	1959–2006, (1967–1979 reconstructed)	Annual

Note. ZK = Zong Kong; GMB = glacier mass balance; ELA = equilibrium line altitude.

accumulation and ablation are equal over a given period, that is, where the mass balance over that period is zero (Dong et al., 2012). The ELA of each hydrological year was here determined by stake observations as well, where the GMB is 0, and derived by the GMBs of individual elevation zones. The annual GMB and ELA are available from 1959 to 1966, and from 1980 to 2006. Data for the 1967–1979 period were reconstructed based on the relationship between summer air temperature and mass balance during 1959–1966 (Zhang, 1981; Table 1).

2.3 | Hydro-meteorological data

Daily runoff data from two gauging stations (No. 1 and ZK; Figure 1) were available during the main snow/glacier melt period (June–August) from 1985 to 2004 (Table 1). Meteorological data were available from the DXG meteorological station located at 3,539 m a.s.l., about 3-km downstream of the glacier (Figure 1) for the period 1958–2006 (Table 1). The long-term average mean daily air temperature is −5.1 °C, with −20 °C in winter and about 0 °C from June to August. Annual average precipitation is 450 mm/a in DXG meteorological station (Ye et al., 2005). Over 90% of precipitation occurs between April and September. Between March 1987 and February 1988, Yang, Zhang, and Zhang (1992) conducted an intensive snow survey close to the DXG meteorological station. Daily snow depth and snow density were measured, from which the snow water equivalent (SWE) was derived.

In the absence of more detailed observations, potential evaporation (E_0) was estimated by the Hamon equation (Hamon, 1961), which only requires daily average tempearture as input data. This was here judged acceptable, as hydrograph simulation has been previously shown to be rather insensitive to different methods of estimating potential evaporation (e.g., Oudin, Michel, & Anctil, 2005). In the study region, the potential evaporation reaches a long-term average of about 200 mm/a. Sublimation from the snowpack may play a role in this cold region, but its importance remains controversial, as illustrated by highly variable estimates. For example, Pomeroy and Essery (1999) found that during blowing snow 10–50% seasonal snow cover was returned to atmosphere as sublimation flux in a North American prairie and arctic case study. In contrast, Zhou, Zheng, Zhou, Dai, and Li (2012) found that sublimation was lower at a study site in Central Asia, which is close to this study site. Due to the scarce data in the study region and the rather incomplete understanding of the process, our model does not take sublimation into account.

3 | MODEL DESCRIPTION

On the basis of the semidistributed conceptual FLEX-Topo modelling framework (Gao, Hrachowitz, Fenicia, et al., 2014; Gharari et al., 2014; Savenije, 2010), we improved the existing FLEX model to include the glacier component (FLEX^G), by integrating snow and glacier components. The FLEX-Topo modelling framework discretizes the studied catchment based on landscapes, with flexible model setups to consider different runoff generation mechanisms on different landscapes. The FLEX modelling framework/philosophy is based on the idea that we need to adapt and customize our models to different environmental conditions (Fenicia, Kavetski, & Savenije, 2011; Fenicia et al., 2008). Due to the distinct runoff generation mechanisms in glacier and nonglacier areas, a parallel model structure was designed to adequately capture the different hydrological behaviours of these two landscape units. The details are shown below.

3.1 | Snow melt simulation

Precipitation is considered as solid (i.e., snow; P_s) or liquid (i.e., rain; P_l) depending on whether the daily average air temperature (T) is above or below a threshold temperature, T_t [°C] (Equations 2 and 3).

$$P_s = \begin{cases} P; & T \le T_t \\ 0; & T > T_t \end{cases}, \tag{2}$$

$$P_l = \begin{cases} P; & T > T_t \\ 0; & T \le T_t \end{cases}. \tag{3}$$

The T_t is a critical parameter (Berghuijs, Woods, Hutton, & Sivapalan, 2016) therefore setting its prior range is essential for calibration. From over 600 in situ observation of meteorological stations in China, Han, Chen, Liu, Yang, and Wenwu (2010) found that T_t ranges from 1 to 5 °C. And this prior range was also supported from other large-sample observation (Kienzle, 2008) and world-wide modelling studies (Martinec, Rango, Roberts, Baumgartner, & Apfl, 1998; Wen, Nagabhatla, Lü, & Wang, 2013). However, there were also other modelling studies in Nordic regions with prior range of (−2.5 to 2.5 °C; Seibert, 1997). In this study, we chose a wider range of T_t (−2.5 to 5 °C) to test its influence on the model skill to reproduce the hydrograph, as well as and snow and ice dynamics.

In addition, due to systematic errors in measuring, mainly caused by wind-induced undercatch, snowfall is typically underestimated (Goodison, Louie, & Yang, 1997; Yang et al., 2001). According to field observations, Yang, Jiang, Zhang, and Kang (1988) concluded that only

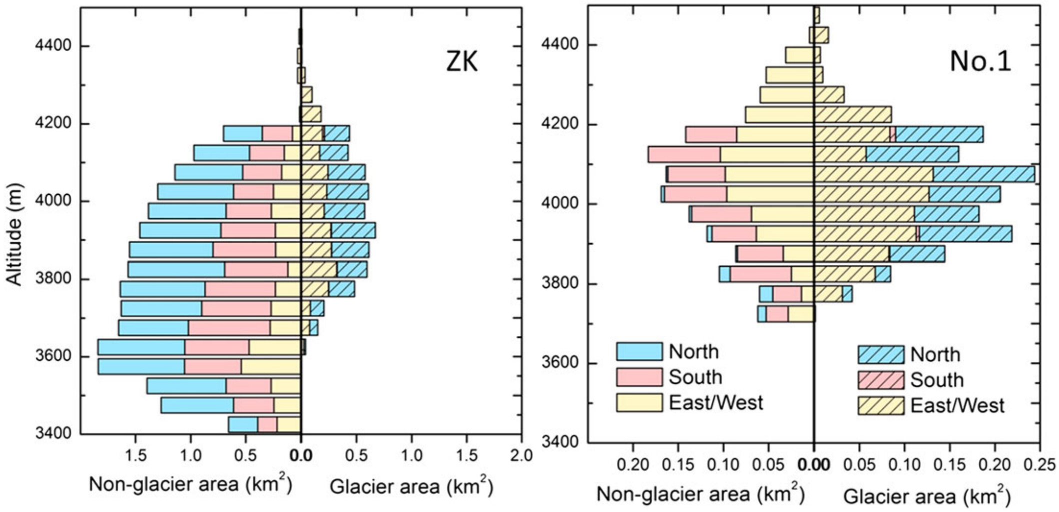

FIGURE 2 Model structure of FLEX^G. The red abbreviations indicate parameters, and black abbreviations indicate storage components and fluxes. Precipitation (P) is considered to be snow (P_s) or rain (P_l) depending on whether the daily average air temperature (T) is above or below a threshold temperature, T_t [°C]. The solid snow pack (S_w) and the liquid water inside the snow pack (S_{wl}) were regarded as separate reservoirs. R_{rf} (mm/day) is the refreezing water from S_{wl} to S_w; M_s (mm/day) indicates the melted snow. P_e (mm d^{-1}) is the generated runoff to soil/ice surface. Snowmelt is calculated on basis of a degree-day factor F_{dd} (mm·°C^{-1}·day^{-1}). The liquid water in the S_{wl} from meltwater and rainfall is retained within the snowpack until it exceeds a certain fraction, C_{wh} (−), of S_w. F_{rr} (−) indicates the correct factor to simulate liquid water refreezing, whereas temperature is below T_t. S_g is the storage of water in the glaciers, which has no limit. M_g (mm/day) represents glacier runoff. F_{dd} is multiplied by C_g to represent the larger amount of glacier than snow with the same air temperature. M_g is then, together with P_l routed through a linear reservoir $S_{f,g}$, controlled by a recession parameter $K_{f,g}$ (day), to compute the runoff generated from glacier areas. For the nonglaciarized area, the unsaturated reservoir (S_u) is used to split the P_e (mm/day) to generated runoff R_u (mm/day) and the infiltration by two free parameters $S_{u,max}$ (mm) and β (−). C_e (−) controls the relationship between soil moisture and actual evaporation. R_u recharges to two linear reservoirs (S_f and S_s) by a parameter (D) to represent the response processes of subsurface storm flow Q_f (mm/day) and groundwater runoff Q_s (mm/day), with to recession parameters K_f (day) and K_s (day). The influence of aspect on snow and ice melting is taken into account by a multiplier C_a (−)

76.5% of the snow falling is captured by observation at this study site. The observations were therefore adjusted with a lumped bias-correction factor of 1.3 (Yang et al., 1988; Yang et al., 2012).

In the temperature-index-based snow model (e.g., Berghuijs et al., 2016; Braithwaite & Olesen, 1989; Hock, 2003; Singh, Kumar, & Arora, 2000; Figure 2) in this study, the snow pack was conceptualized as a porous media which can hold liquid water from melting/rainfall and where the liquid water can refreeze (Fujita & Sakai, 2014). Therefore, the solid snow pack (S_w) and the liquid water inside the snow pack (S_{wl}) were regarded as separate reservoirs. The water balance of the S_w reservoir is shown in Equation 4, where R_{rf} (mm/day) is the refreezing water from liquid storage (S_{wl}) to solid storage (S_w) and M_s (mm/d) indicates the melted snow. Equation 5 shows the water balance of liquid water (S_{wl}) in snow pack, where P_e (mm/day) is the generated runoff to soil/ice surface. Note that the SWE is the sum of solid (S_w) and liquid water (S_{wl}), stored in snow pack.

Snowmelt is calculated on basis of a degree-day factor F_{dd} (mm·°C^{-1}·day^{-1}) to calculate melt water by the temperature T (°C) above the threshold temperature T_t (°C). The prior range of F_{dd} was set as (4–10 mm [°C day]$^{-1}$), obtained from numerous field-based measurements in China (Zhang et al., 2006). The liquid water in the S_{wl} from meltwater and rainfall is retained within the snowpack until it exceeds a certain fraction, C_{wh} (−), of the solid SWE (S_w; Equation 7; Konz et al., 2007; Seibert, 1997; Yang et al., 2012). Liquid water within the snowpack refreezes according to Equation 8. F_{rr} (−) indicates the correct factor to simulate liquid water refreezing, whereas temperature is below T_t (Seibert, 1997; Konz et al., 2007; Yang et al., 2012). It is worthwhile to note that snow accumulation/melt is calculated for each individual elevation zones rather than in a lumped way, which is further described in Section 3.4.

$$\frac{dS_w}{dt} = P_s + R_{rf} - M_s, \tag{4}$$

$$\frac{dS_{wl}}{dt} = P_l + M_s - R_{rf} - P_e, \tag{5}$$

$$M_s = \begin{cases} F_{dd}(T - T_t); & T > T_t \\ 0; & T \leq T_t \end{cases}, \tag{6}$$

$$P_e = \begin{cases} S_{wl} - C_{wh}S_w; & S_{wl} > C_{wh}S_w \\ 0; & S_{wl} \leq C_{wh}S_w \end{cases}, \tag{7}$$

$$R_{rf} = \begin{cases} F_{dd}F_{rr}(T_t - T); & T_t > T \\ 0; & T_t \leq T \end{cases}. \tag{8}$$

3.2 | Glacier melt simulation

The glacier component is, as the snow model above, based on a temperature-index model. If the ice is covered by snow, the energy is first provided to melt snow. If there is no snow cover, the ice starts to melt, generating glacier runoff M_g (mm/day; Equation 9). Note that the degree-day factor for glaciers is assumed to be larger than the snow degree-day factor in the same region (Braithwaite & Olesen, 1989; Seibert, Jenicek, Huss, & Ewen, 2015), mainly due to the lower albedo of ice. Its prior range is also obtained from field-based observation (Zhang et al., 2006) and previous modelling studies (Yang et al., 2012). This was here accounted for by the multiplier C_g. M_g is then, together with P_l routed through a linear reservoir $S_{f,g}$, controlled by a recession parameter $K_{f,g}$ (day), to compute the runoff generated from glacier areas (Equations 10 and 11). The modelled annual GMB estimates were then derived from the glacier and snow pack simulations in individual elevation and aspect zones (detailed method is described in Section 3.4). Similarly, the annual ELA was estimated by the annual GMBs of individual elevation zones, in which the annual GMB is 0, and ablation is equal to accumulation. It is worthwhile to note that both the measured and the calculated annual GMB are shown as water equivalent.

$$M_g = \begin{cases} F_{dd}C_g(T - T_t); & T > T_t \text{ and } S_w = 0 \\ 0; & T \leq T_t \text{ or } S_w > 0 \end{cases}, \tag{9}$$

$$\frac{dS_{f,g}}{dt} = P_l + M_g - Q_{f,g}, \tag{10}$$

$$Q_g = S_{f,g}/K_{f,g}. \tag{11}$$

3.3 | Nonglacier area rainfall–runoff simulation

Rainfall and snow melt, estimated from the snow, enter the unsaturated reservoir (S_u), characterized by

$$\frac{dS_u}{dt} = P_e - E_a - R_u, \tag{12}$$

where P_e (mm/day) is the effective rainfall, that is, snow melt and rainfall; E_a (mm/day) is the actual evaporation, which was estimated based on potential evaporation (E_0) and relative soil moisture ($S_u/S_{u,max}$), with a free parameter C_e (−; Equation 13); R_u (mm/day) is the water that exceeds the storage capacity and cannot be stored in S_u, determined by the Xinanjiang storage capacity curve (Equation 14; Zhao & Liu, 1995).

$$E_a = E_0 \frac{S_u}{C_e S_{u,\max}}, \tag{13}$$

$$\frac{R_u}{P_e} = 1 - \left(1 - \frac{S_u}{(1+\beta)S_{u,\max}}\right)^{\beta}, \tag{14}$$

where $S_{u,max}$ (mm) represents the root zone storage capacity and β (−) is the shape parameter. Excess water from S_u, that is, R_u, recharges two linear reservoirs (S_f and S_s) by a parameter (D) to represent the response processes of subsurface storm flow Q_f (mm/day) and groundwater runoff Q_s (mm/d):

$$\frac{dS_f}{dt} = R_f - Q_f, \tag{15}$$

$$\frac{dS_s}{dt} = R_s - Q_s, \tag{16}$$

$$Q_f = S_f/K_f, \tag{17}$$

$$Q_s = S_s/K_s, \tag{18}$$

where R_f (mm/day) is the recharge into the fast response reservoir obtained by R_u·D and R_s (mm/day) is the recharge into the slow response reservoir obtained by R_u·(1 − D); K_f (day) is the fast recession parameter and K_s (day) is the slow recession parameter.

3.4 | Accounting for topography

The areal representativeness of point meteorological observations is, due to elevation and shading effects, a pervasive problem in mountainous regions (e.g., Hrachowitz & Weiler, 2011; Klemeš, 1990). Most meteorological stations are located in valleys at relatively low elevations to allow good access for maintenance (e.g., Stahl, Moore, Floyer, Asplin, & McKendry, 2006), which typically introduces an elevation bias in the observed variables. To offset these biases, temperature in the individual elevation zones was here adjusted with an environmental lapse rate of −0.007 °C/m (Li, Wang, et al., 2013; Yang et al., 2012), for both potential evaporation and snow/ice relevant calculation. Although precipitation was corrected for with a locally suitable lapse rate of 0.05%/m, which was obtained by field observations (Yang et al., 1988; Yang et al., 2012).

As topography has considerable influence on the spatial forcing data distribution and the energy budget (e.g., Euser et al., 2015), it does consequently also influence spatial–temporal variations in glacier and snow dynamics. This is, besides elevation, in particular true for aspect as direct solar radiation is a first-order control on snow/ice melt (Hock, 2005). To account for these influences, although balancing accuracy and data availability with computational cost, the catchments in this study were stratified in 50-m elevation zones, resulting in a total of 16 elevation zones in the glacier no. 1 and 21 in the ZK catchment. Each elevation zone was then further divided into three aspect zones, that is, north (315°–45°), south (135°–225°) as well as the east/west (45°–135° and 225°–315°) facing aspects. In summary, considering different elevations, aspects as well as glacier and nonglacier areas, the glacier no. 1 and ZK catchments were classified into 96 and 126 classes, respectively (Figure 3). Due to the lack of detailed energy balance observations, the influence of aspect on snow (Equation 19) and ice (Equation 20) dynamics is taken into account by a conceptual multiplier C_a (−), which is larger than 1. The F_{dd} in south facing aspects are multiplied by C_a, and the north facing aspects are multiplied by $1/C_a$, and the east/west facing aspects are kept as F_{dd}.

$$M_s = \begin{cases} F_{dd}C_a(T - T_t); & T > T_t \\ 0; & T \leq T_t \end{cases}, \tag{19}$$

$$M_g = \begin{cases} F_{dd}C_aC_g(T - T_t); & T > T_t \text{ and } S_w = 0 \\ 0; & T \leq T_t \text{ or } S_w > 0 \end{cases}. \tag{20}$$

4 | MODEL EVALUATION, CALIBRATION, EVALUATION, AND TRANSFERABILITY

A Monte Carlo sampling strategy with $5{\cdot}10^5$ realizations from uniform prior parameter distributions, as obtained from literature (Table 2). together with a multiobjective calibration strategy (e.g., Euser et al., 2013) was chosen to obtain posterior distributions of the 13 free model parameters. Besides the hydrograph, snow and ice accumulation and ablation are essential components of modelled system. Therefore, the model parameters were calibrated using all available data for the study region: daily runoff for the period 1985–1994, daily estimates of SWE for the period March 1987–February 1988, annual estimates

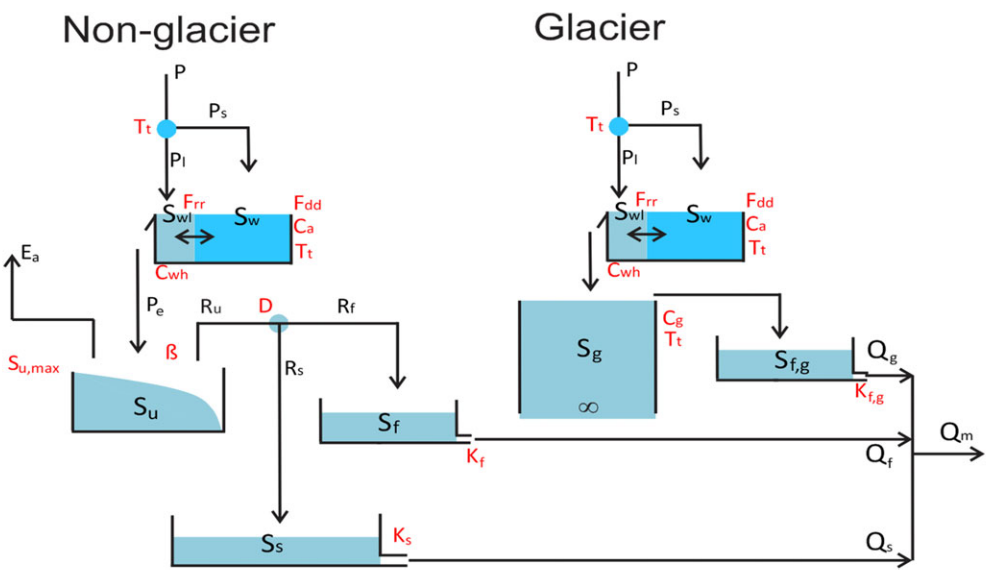

FIGURE 3 Area of different elevation and aspects of the glacier region and the nonglacier region in the Zong Kong (ZK) catchment and the No. 1 catchment

TABLE 2 Model parameters and their prior ranges for Monte Carlo sampling in GLUE method

Parameters	Description	Unit	Prior range	Method to estimate
T_t	Threshold temperature to split snowfall and rainfall	°C	(−2.5, 5)	(Han et al., 2010; Kienzle, 2008; Martinec et al., 1998; Seibert, 1997)
F_{dd}	Degree-day factor of snow	mm (°C day)$^{-1}$	(4, 10)	(Zhang et al., 2006; Yang et al., 2012)
C_g	Factor for ice melt	–	(1, 2)	(Gao, He, Ye, & Pu, 2012)
C_a	Factor for the influence of aspect on melt	–	(1, 2)	(Gao et al., 2012)
C_{wh}	Snow water holding capacity	–	(0, 1)	(Gao et al., 2012)
F_{rr}	Refreezing factor	–	(0, 1)	(Gao et al., 2012)
$K_{f,g}$	Recession coefficient of glacier runoff	days	(1, 5)	(Gao et al., 2012)
$S_{u,max}$	Root zone storage capacity	mm	(30, 120)	(Gao et al., 2012; Gao et al., 2014)
β	Shape parameter	–	(0.1, 1)	(Gao et al., 2012)
C_e	Evaporation threshold value	–	(0.1, 0.7)	(Gao, Hrachowitz, Fenicia, et al., 2014)
D	Splitter	–	(0, 1)	(Gao, Hrachowitz, Fenicia, et al., 2014)
K_f	Recession coefficient of fast response reservoir	days	(1, 15)	(Gao, Hrachowitz, Fenicia, et al., 2014)
K_s	Recession coefficient of slow response reservoir	days	(15, 200)	(Gao, Hrachowitz, Fenicia, et al., 2014)

Dash means the parameter is dimensionless without unit.

of the GMB for the period 1959–2006, and annual estimates of ELA for the 1959–2006 period. The weighted sum was then used as objective function (I_{KGE_HGS}), to combine the four objectives into one metric, giving different weights to runoff (I_{KGE_H}), SWE (I_{KGE_SWE}), GMB (I_{KGE_GMB}), and ELA (I_{KGE_ELA}; Equation 21).

$$I_{KGE\_HGS} = 0.7I_{KGE\_H} + 0.1I_{KGE\_GMB} + 0.1I_{KGE\_ELA} + 0.1I_{KGE\_SWE}, \quad (21)$$

where the performance of hydrograph was given the highest weight (0.7) due to the elevated information content in the 20-year time series of runoff data, as compared to the much shorter time series and/or lower temporal resolution of available data for the other three model objectives. The Kling–Gupta efficiency (Gupta, Kling, Yilmaz, & Martinez, 2009; I_{KGE}) was used as performance metric for the individual objectives:

$$I_{KGE} = 1-\sqrt{(r-1)^2 + (\alpha-1)^2 + (\beta-1)^2}, \quad (22)$$

where r is the linear correlation coefficient between simulation and observation; α ($\alpha = \sigma_m/\sigma_o$) is a measure of relative variability in the simulated and observed values, where σ_m is the standard deviation of simulated variables and σ_o is the standard deviation of observed variables; β is the ratio between the average value of simulated and observed variables. The 1% (5,000) best performing parameter sets were retained as behavioural and used to establish feasible posterior distributions and to construct model uncertainty ranges, using I_{KGE_HGS} as informal likelihood measure (GLUE; Beven & Binley, 1992; Freer, McMillan, McDonnell, & Beven, 2004; Shafii, Tolson, & Shawn, 2015; Zhang, Li, Guo, & Gong, 2015).

Traditional split-sample validation was used, to test the models ability to reproduce the observed hydrograph for a different period (1995–2004). As an additional, potentially more rigorous model test, the calibrated FLEX^G model from the nested 3.3 km^2 glacier no. 1 subcatchment was then transferred and up-scaled without further calibration to the 28.9 km^2 downstream ZK catchment (Figures 1 and 2) and evaluated for its skill to reproduce the hydrological response in that catchment for the 1985–2004 period. More specifically, the model was run in the ZK catchment with the feasible parameter sets obtained from calibration in the glacier no. 1 catchment. To account for the differences in landscape structure between the two catchments, the elevation distributions as well as the proportions the individual aspect classes and, most importantly, the proportions of glacier and nonglacier area were adjusted according to Figure 2.

In the absence of additional SWE, GMB and ELA data for the model validation and transfer/up-scaling the model was evaluated based on I_{KGE_H}, using runoff data from the ZK catchment. In addition, to allow for a comprehensive evaluation, three more performance criteria, that is, bias error (I_{BIAS}), root mean square error (I_{RMSE}), and Nash–Sutcliffe efficiency (I_{NSE}), were used:

$$I_{BIAS} = \frac{1}{n}\sum_{t=1}^{n}\left(Q_{m,t} - Q_{o,t}\right), \tag{23}$$

$$I_{RMSE} = \sqrt{\frac{\sum_{t=1}^{n}\left(Q_{m,t} - Q_{o,t}\right)^2}{n}}, \tag{24}$$

$$I_{NSE} = 1 - \frac{{I_{RMSE}}^2}{\sigma_o^2}. \tag{25}$$

5 | RESULTS AND DISCUSSION

5.1 | Hydrological simulation

Figure 4 shows that the observed hydrograph of the glacier no. 1 catchment is well reproduced and enveloped by the 5%/95% uncertainty interval by FLEX^G model, in both calibration (1986) and validation (2001) period. The model performance of the entire periods from 1985 to 2004 is shown in Figure S1. In 57% of the time steps, the observations are within the generally well constrained uncertainty interval. The average I_{KGE_HGS} of all behavioural parameter sets is 0.49 in calibration. The average I_{KGE_H} of all behavioural parameter sets is 0.74 in calibration (with the 5%/95% uncertainty range of 0.70–0.78), and 0.73 in validation, whereas I_{BIAS} in validation is limited to −0.55 mm/day (−6%), I_{RMSE} = 3.58 mm/day, and I_{NSE} = 0.61 (Table 3).

To understand the hydrological behaviour of glacier and nonglacier areas, we separated the hydrograph of the glacier no. 1 catchment into two respective components (Figures 4, S1). It can be seen that the hydrograph in general, and in particular during peak flow conditions, is dominated by the glacier area (52%), contributing 80% of the total runoff; whereas the nonglacier area that covers ~48% of the catchment contributes only 20% to the total runoff. As glacier melt is mainly controlled by the energy input, this illustrates that in the study area direct precipitation has limited influence on runoff generation

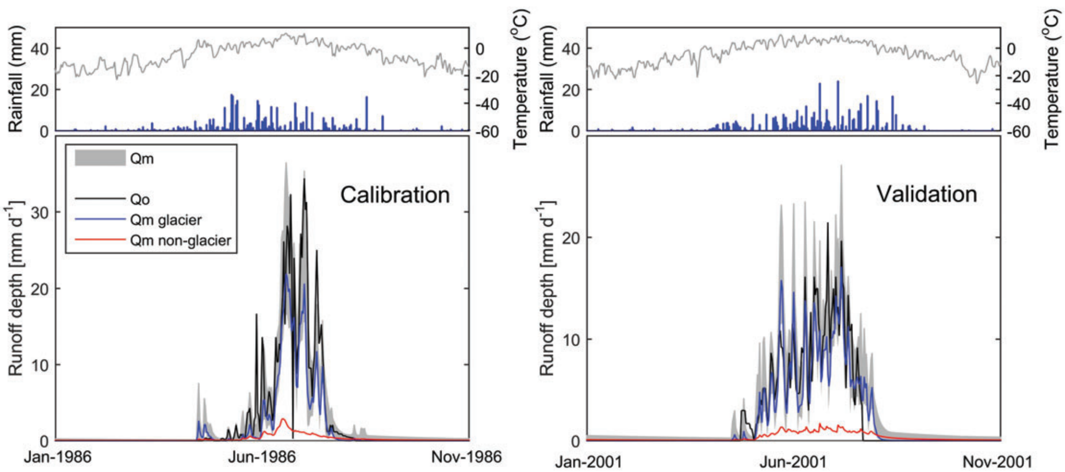

FIGURE 4 Glacier no. 1 catchment. The upper panels show the observed daily average air temperature (grey line) and daily precipitation (blue bars) for two selected time periods; the lower panels show the comparison between observed (black line) and the modelled 5%/95% uncertainty intervals of daily runoff (grey shaded areas) and the respective contributions from glacier (blue) and nonglacier (red) parts of the catchment (averaged value from all behavioural parameter sets). The left figure shows part of results during the calibration period. The right figure shows part of the results for the independent test, that is, validation, period. The results of the complete modelling time series are provided in Figure S1, and monthly results are shown in Figure S5

TABLE 3 The performance of FLEX^G and FLEX^{G_nA} in validation and transferability with different criteria

	Calibration	Validation				Transferability			
	I_{KGE_HGS} (−)	I_{KGE_H} (−)	I_{BIAS} (mm/day)	I_{RMSE} (mm/day)	I_{NSE} (−)	I_{KGE_H} (−)	I_{BIAS} (mm/day)	I_{RMSE} (mm/day)	I_{NSE} (−)
FLEX^G	0.49	0.73	−0.55	3.58	0.68	0.55	0.39	2.54	0.47
FLEX^{G_nA}	0.48	0.72	−0.59	3.68	0.64	0.43	0.58	2.76	0.38

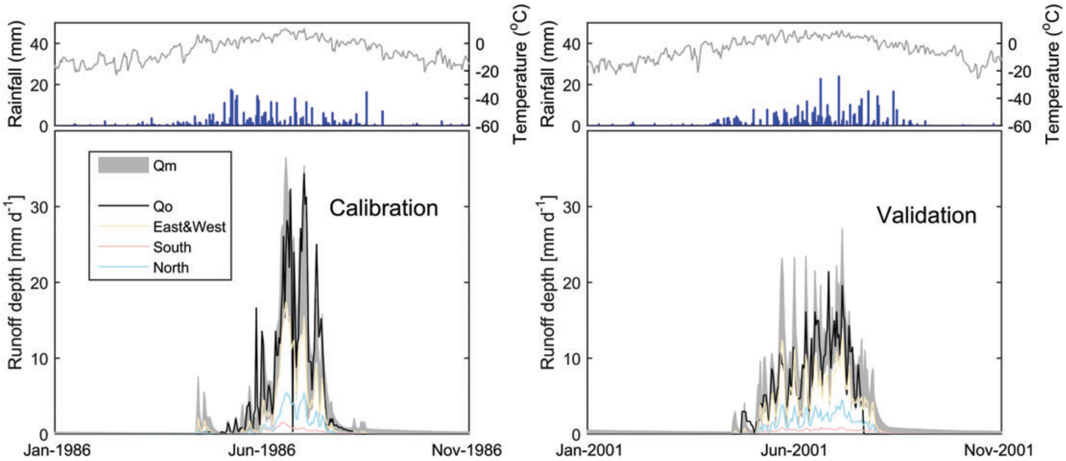

FIGURE 5 The observed daily average air temperature (grey line) and daily precipitation (blue bars) and the comparison between observed (black line) and the modelled 5%/95% uncertainty intervals of daily runoff (grey shaded areas), runoff generated on east/west, south or north facing aspects (averaged value from all behavioural parameter sets) in the glacier no. 1 catchment. The left figure shows the results from a part of the calibration period. The right figure shows the results for part of the validation period. The results of the complete modelling time series are provided in Figure S2, and monthly results are shown in Figure S6

compared to temperature. And that the glaciers contribute around 4 times runoff per unit area compared with the non-glacier area.

Figures 5 and S2 show the individual modelled hydrograph components for north, south, and east/west aspects. The results illustrate that east/west facing regions contribute the dominant proportion of runoff, although its areas are comparable with the north-facing regions (see Figure 3). North-facing hillslopes contribute the second largest runoff proportion, likewise due to their large glacier area, in spite of reduced snow/ice melt due to lower direct incoming radiation, conceptualized here by the lower degree-day factor. The south facing hillslopes generate limited amount of runoff, due to the lack of glacier to contribute continuous runoff without rainfall. This result clearly highlights the significant impact of aspect on glacier distribution and runoff generation.

In addition and as a further evaluation metric, Figure 6 shows that the FLEX^G model can adequately reproduce the flow duration curve of the catchment for both high flow, and low flow is slightly underestimated.

5.2 | Glacier and snow simulation

Figure 7 shows the comparison between observed and FLEX^G modelled GMB and ELA. It can be seen that the 5%/95% model uncertainty interval envelops a considerable proportion of the observations (70% and 67%, respectively), with average I_{KGE_GMB} for 0.33 and I_{KGE_ELA} for 0.25, respectively, except for the periods between 1967 and 1979, which were reconstructed from meteorological data. From the observed GMB, we found that the no. 1 glacier has experienced severe ablation, in particular after 1994, which was well reproduced by the model. Simultaneously the ELA exhibits a significant upwards trend, particularly from 1994 onwards ($p < .05$), with the increase of about 4.5 m/year. This is in line with an observed general increase of air temperature over the observation period in the study region (Li et al., 2010). The modelled average GMB was −483 mm/a, which is a 130 mm/a overestimation of ice water equivalent loss compared with the observed GMB (−353 mm/a), whereas the modelled ELA was on average 33 m higher than the observations.

Although the FLEX^G model reproduced the GMB and ELA quite well from the 1990s on, the systematic underestimation of GMB and overestimation of ELA in the 1960s likely indicates the effect of a decreasing glacier albedo due to dust accumulation in this region (Huang et al., 2010; Ming, Xiao, Du, & Yang, 2013), which is not accounted for in the time-invariant parameterization of the snow- and glacier-related parameters in this model, resulting in an underestimation of albedo in the 1960s. The lack of long-term albedo observation (Wang, Ye, Cui, He, & Yang, 2014) prevents a meaningful parameterization of this process in the FLEX^G model. Another interpretation is the neglecting of possible snow redistribution caused by the blowing snow from nonglacier areas to the glacier covered area, which likely influences on GMB and ELA (Dadic, Mott, Lehning, & Burlando, 2010; Schirmer, Wirz, Clifton, & Lehning, 2011; see also in Section 5.3).

Figure 7 shows both the observed and modelled glacier volume has been experiencing severe thinning and mass loss. This can explain the remarkable larger runoff generated from glacier area. Another supporting evidence is that the hydrograph does not follow the change of precipitation but rather the variation of temperature. The runoff depth of peak flow is often even higher than the amount of precipitation, resulting in both observed and modelled runoff coefficients larger than 1 (see details in Section 5.3). This supports, in our opinion, the assumption of severe ice melting and loss which contribute to the runoff yield and shape the hydrograph in this specific study area.

The modelled area-averaged SWE of the elevation range with south facing aspect in which the snow survey was done (Figure 8). without considering spatial variability in SWE, roughly reproduces the general features of the observed snow accumulation and ablations variation (I_{KGE_SWE} = 0.61) for the March 1987 to February 1988, the period for which SWE observation was available. Interestingly, in the early melt period in 1987 the uncertainty is quite large. This is here, besides other factors which can reduce the representativeness of this plot-scale snow survey (Clark, Hendrikx, et al., 2011; e.g., snow drift),

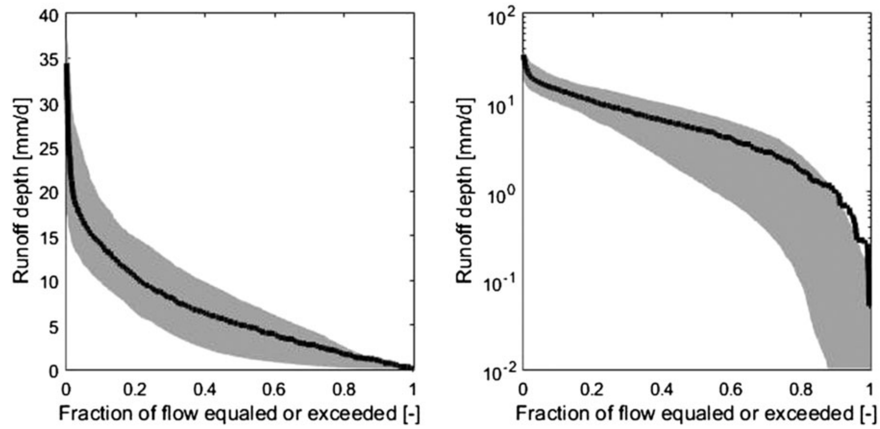

FIGURE 6 Simulated (5%/95% limits are shown by grey shaded areas) and observed (black line) flow duration curve in the glacier no. 1 catchment

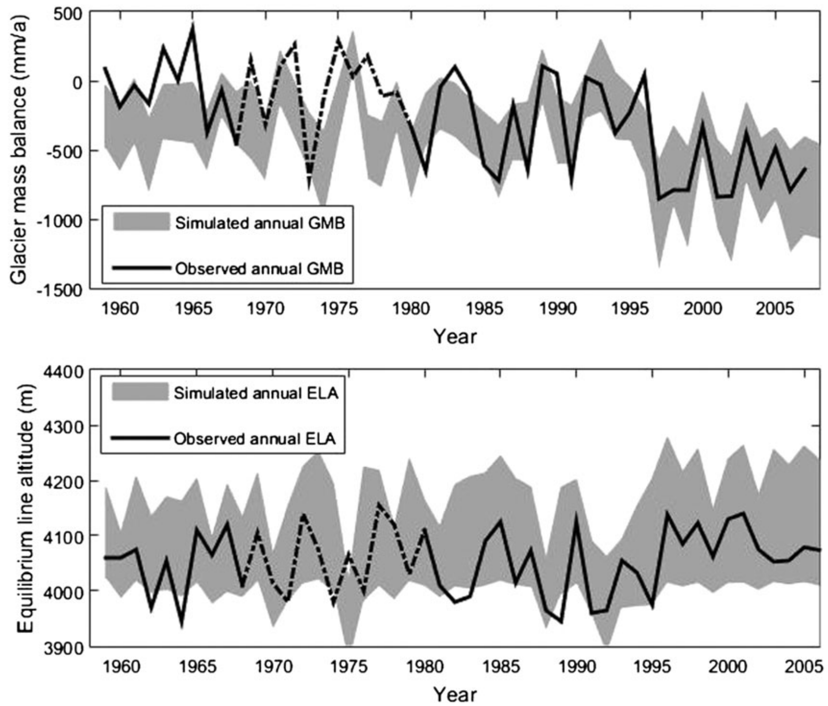

FIGURE 7 Glacier no. 1 catchment. Upper panel shows the modelled and observed glacier mass balance (GMB). Lower panel shows modelled and observed equilibrium line altitude (ELA). Dashed lines represent the GMB and ELA reconstructed from meteorological data from 1967 to 1979; 5%/95% uncertainty limits are indicated by the grey-shaded areas

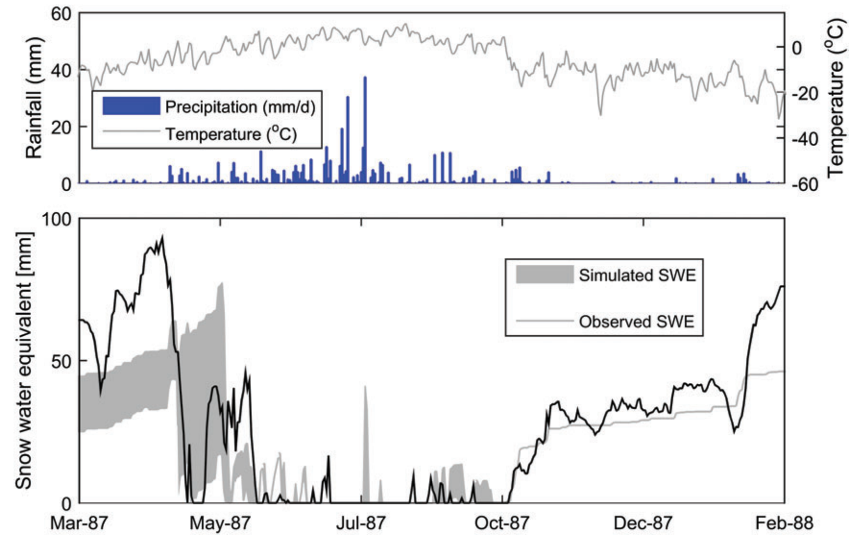

FIGURE 8 The comparison between the 5%/95% uncertainty interval of the modelled (grey-shaded area) and the observed (black line) daily snow water equivalent from March 1987 to February 1988, as well as the observed daily average air temperature (grey line) and precipitation (blue bars)

mostly linked to the influence of the threshold temperature (T_t). The temperature during precipitation events in the early winter of 1986/1987 was close to the threshold temperature. Therefore, the different feasible T_t values obtained from calibration to stream flow, strongly influenced the development of the snow pack. However, during the precipitation events in the early winter of 1987/1988 the air temperature dropped sharply, which led to the well constraint uncertainty in estimating the SWE.

5.3 | Water balance

The annual averaged water balance for the glaciated and nonglaciated areas of the no. 1 catchment were analysed. In nonglacier covered region, the long-term annual precipitation was 539 mm/a, with actual evaporation at around 170 mm/a (with 5%/95% uncertainty of 96–223 mm/a), annual runoff of 289 mm/a (201–382 mm/a), and 80 mm/a (58–97 mm/a) water that accumulates as snow but does not melt even at high elevation during summer. Interestingly, in nonglacier area, according to field surveys, there is no evidence of permanent snow cover at high elevations. In the glacier area, the annual averaged precipitation was 578 mm/a, modelled annual averaged runoff 1,061 mm/a (885–1217 mm/a), 483 mm/a (303–659 mm/a) of which was contributed by glacier thinning as indicated by the loss in the GMB. The averaged simulated GMB is 130 mm/a more than the observed GMB. The overestimation of ice loss in the glacier area and the modelled but not observed snow accumulation in nonglacier area is a strong indication of snow redistribution by snow drifting, sloughing, or even avalanches from nonglacier area to glacier areas (Anderton et al., 2004; Blöschl et al., 1991; Clark, Hendrikx, et al., 2011), which is not accounted for in the model. This is a hypothesis that needs to be tested by field measurement in this region, in particular including wind field analysis, for example, the wind exposure and shelter proposed by Winstral and Marks (2002).

5.4 | Parameter identification

From the dotty plots of behavioural parameters in Figure 9, it was found that several parameters were quite well identified, including T_t, C_a, $K_{f,g}$, and D. T_t is well constrained because it controls the dominant process in the region, that is, the partitioning of rainfall, snowfall, and the threshold temperature for snow and ice melt. C_a reflects the impact of different aspects on melting. We found that it is also rather well constrained, which indicates the sensitivity of the hydrograph as well as of the snow and ice dynamics to aspect, which well represented by this conceptual parameter. $K_{f,g}$ determines the recession process in the glacier area, which implies its considerable influence on the shape of hydrograph. The well-constrained snow- and ice-related parameters illustrated that here the hydrograph contains considerable information from snow and glacier processes, which is not a surprise, given the snow/ice melt dominated regime. Besides that, D controls

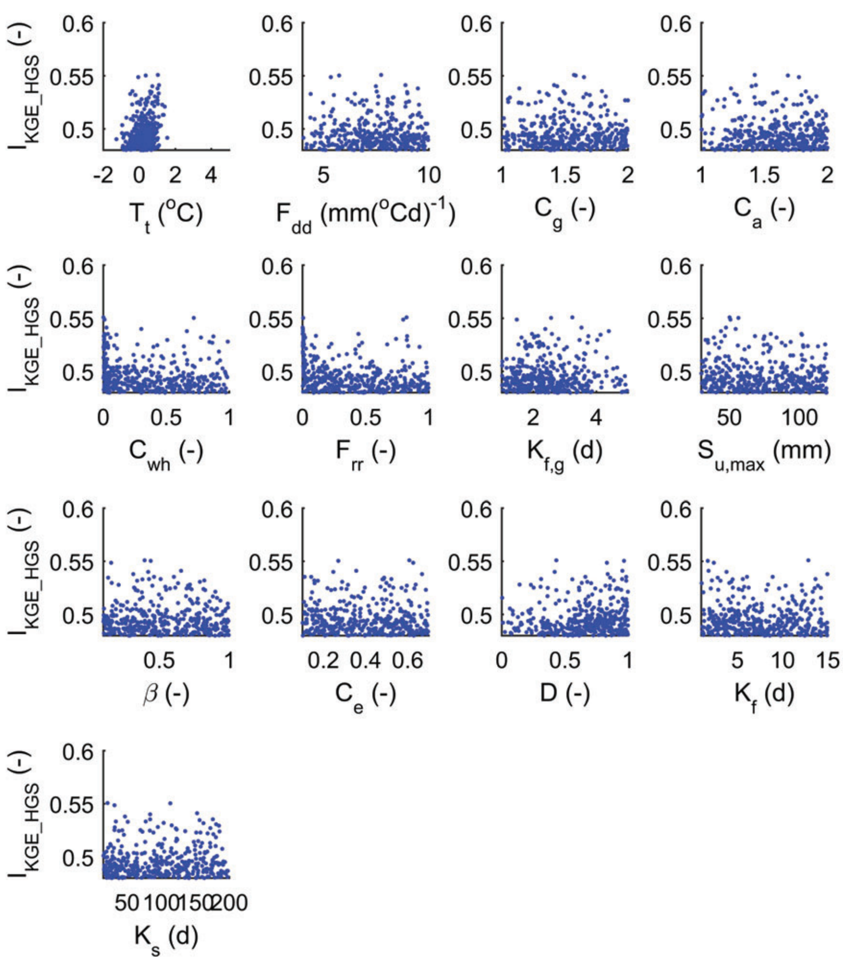

FIGURE 9 Dotty plots of the individual sets of behavioural parameters against I_{KGE}

the split of fluxes to the fast and slow response reservoirs in nonglacier areas which strongly influences the shape of the hydrograph.

Other parameters, such as $S_{u,max}$, β, K_f, and K_s, are less well identified. As most of the poorly identifiable parameters are largely associated with the nonglacier area in the catchment, this suggests that the observed hydrograph does not contain sufficient information from that area due to the higher proportion of glacier runoff in total streamflow. The large uncertainty of K_s is mostly likely caused by the lack of flow data in the late recession period (i.e., autumn and winter) as the hydrological field surveys regularly stopped at the end of August.

5.5 | Model transferability and upscaling

The hydrograph obtained from the transferred and up-scaled model for the ZK catchment, is shown in Figures 10 (1986), S3, and S4 (1985–2004). With a mean I_{KGE_H} of 0.55, I_{BIAS} as 0.39 mm/day, I_{RMSE} as 2.54 mm/day, and I_{NSE} as 0.47 over the 20 modelled years (1985–2004), the FLEX^G model captures the general dynamics of the hydrograph in the ZK catchment reasonably well, which is in particular true for the timing and flow magnitudes at the onset of the melt periods in early summer where most observations fall well within the modelled 5%/95% uncertainty bounds. It was, however, also observed that, although still adequately reproducing the general variation, the model increasingly and consistently overestimates flow later in the melt season. The cause of this effect remains unclear at this point but may potentially be related to the overestimation of ice melting or precipitation, or the underestimation of evaporation, for both of which we however do not have sufficient information to underpin these hypotheses. The transferability test nevertheless highlights the value of topographic information for model transferability, providing some evidence that once a suitable characterization of landscape, and thus, hydrological process heterogeneity is accounted for, a model can be relatively robustly up-scaled or transferred to other catchments within climatically similar ecoregions without further calibration. This supports the results of various earlier studies (Gao, Hrachowitz, Fenicia, et al., 2014; Refsgaard et al., 2014). Here, the adequate model upscaling indicates that the model is capable to reproduce hydrographs in the Urumqi glacier no. 1 catchment with different proportions of glacier cover.

The relative contributions to the hydrograph at the ZK station is different from glacier no. 1. Comparing Figure 10 with Figure 4, we can see that a larger proportion of runoff is in the ZK catchment generated from nonglacier area (covered by seasonal snow, much bare rock, and sparse vegetation), due to the larger proportion of nonglacier area in that catchment. It is interesting to find that at the beginning of the melting season, the nonglacier region dominates the runoff generation. With the increase in temperature later in the season, the relative proportion of runoff from the glacier area becomes dominant. In contrast to the glacier no. 1 catchment, flow generated on hillslopes with north facing aspects provides the highest relative contribution to the hydrograph, due to higher proportion of north facing aspect in the ZK catchment. Both in the glacier no. 1 and ZK catchments, east/west and north-facing glaciers are dominant, indicating that topography plays an important role determining the location of glaciers, and the necessity to account aspect in glacier hydrological modelling.

5.6 | Does considering aspect improve model performance?

Subsequently, we tested the impact of aspect on model performance in the Urumqi glacier no. 1 catchment in Central Asia. The FLEX^{G,nA} is a model setup that does not account for aspect but, apart from that, has the same model structure and parametrization as FLEX^G. The only difference is that the degree-day factor in FLEX^{G,nA} is the same in three zones with different aspect, which implies that in this setup aspect does not influence snow and ice melting. We found that when neglecting the influence of aspect, the model's skill to reproduce the hydrograph was not reduced (Figure 11; Table 3). The model's ability

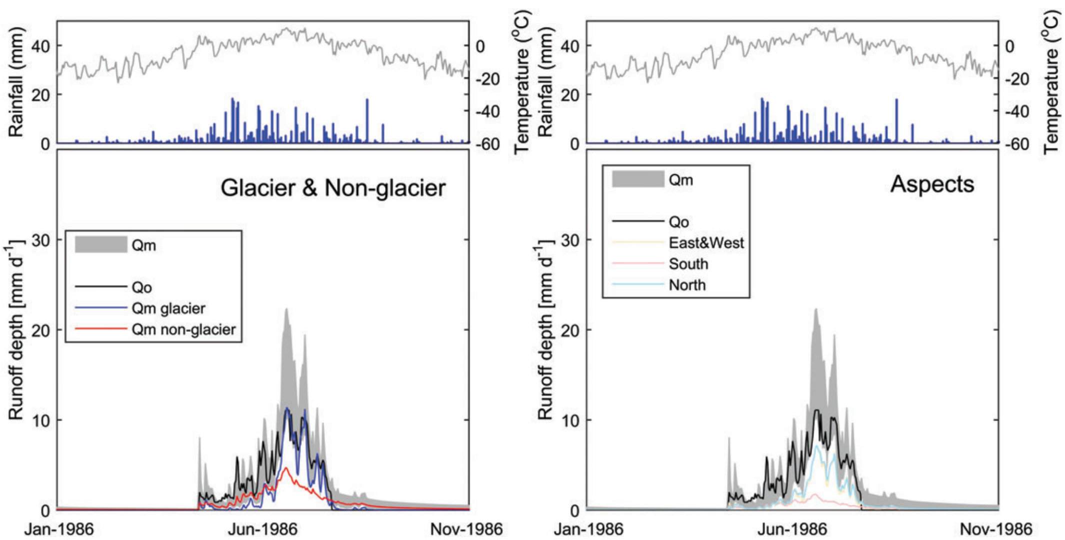

FIGURE 10 Zong Kong (ZK) catchment. Modelled hydrograph and individual contributions from glacier/nonglacier areas as well as from different aspects. The results were obtained by using the parameters calibrated for the glacier no. 1 catchment and adjustment of the areal proportions of glacier/nonglacier areas as well as of the different aspects to the situation in the ZK catchment. The results of the complete modelling time series are provided in the Figures S3 and S4, and monthly results are shown in Figures S7 and S8

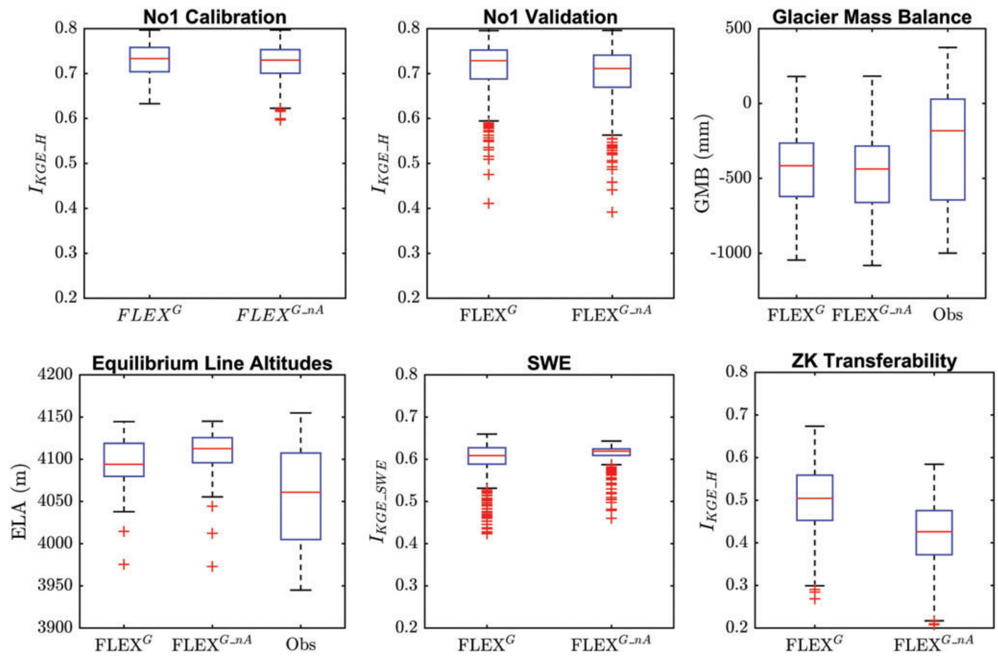

FIGURE 11 Comparison between FLEX^{G} and FLEX^{G_nA} of glacier no. 1 hydrograph calibration, validation, glacier mass balance (GMB) and equilibrium line altitude (ELA) simulation, snow water equivalent (SWE) reproduction, and model transferability from the glacier no. 1 to Zong Kong (ZK) catchment

to mimic the GMB, the ELA, and the SWE was only slightly decreased. However, and most importantly, the spatial model transferability from glacier no. 1 to ZK suffered from considerable reduction in I_{KGE_H} from on average 0.55 to 0.43; I_{BIAS} increased from 0.39 to 0.43 mm/day; I_{RMSE} increased from 2.54 to 2.76 mm/day and I_{NSE} reduced from 0.47 to 0.38 (Table 3). The results illustrate that although the model provides sufficient degrees of freedom to fit the observed data even without considering the aspects (Table 3). accounting for aspects does significantly improve the spatial transferability of the model as it explicitly accounts for the spatial heterogeneity of energy inputs that control the liquid water availability in this snow- and ice-dominated region.

The simulated hydrographs and runoff components from glacier and nonglacier area of both FLEX^{G} and FLEX^{G_nA} are shown in Figure 12. It can be found that although FLEX^{G} has one more parameter than FLEX^{G_nA}, the uncertainty envelope of FLEX^{G} is even narrower than the FLEX^{G_nA}, which implies the more robust simulation of the FLEX^{G} model than FLEX^{G_nA}. From the modelled runoff components of the two models, we found their difference is mainly caused by the different runoff generation from glacier area.

In order to physically explain the better transferability of the FLEX^{G} model, it is worthwhile to explore the different aspect proportions of the glaciers areas in No.1 and ZK catchments. From the aspect information of two nested catchments, we found that in No.1 catchment, glacier with east/west, south, and north aspects cover 29%, 0.8%, and 25%, respectively, of the No.1 catchment. These proportions change to 9%, 0.4%, and 11.6% in the ZK catchment. Furthermore, with one unit glacier area, the No.1 catchment has 52% east/west-facing glaciers, 2% south-facing glaciers, and 46% north-facing glaciers, while in the No.1 catchment the proportions are 43%, 2%, are 55%. Apparently, the two nested catchments have similar proportion of south-facing glaciers, but the ZK catchment (receiver catchment) has larger proportion of north-facing aspect, which generates less glacier runoff. Therefore, without considering the aspect, transferring the FLEX^{G_nA} model and its parameters from the donor no. 1 catchment to the receiver ZK catchment will overestimate glacier melt and runoff in the ZK catchment. This analysis physically demonstrates the advantage of considering aspect in glacier-hydrology model in this glacier catchment in Central Asia, which is in line with previous studies that different aspects result in considerable spatial variations of snow and ice melt (Fujihara et al., 2017; Garvelmann et al., 2015; Pohl et al., 2014) and neglecting the impact of aspect on melt rate in complex terrain is subject to mismatch with site scale measurements (Hock, 1999). It is worth to note that we conceptualized the impact of aspect on snow and ice melting by imposing the higher melt rates on south compared to north slopes by parameter C_a, which still needs to be further tested in the future for feasibility to meaningfully represent the effect of aspect on melting process in the study region.

5.7 | Limitations and outlook

In this study, the area of glaciers was treated as fixed. The temporal variation of areal glacier extent, that is, retreat (or advance) and the associated reduction (or increase) of glacier area, was therefore not explicitly considered in this study. For predictions of future response in the light of climate change, it will, however, be essential to accommodate these processes in the model.

Similarly, time-variant albedo information is worthwhile to be taken into account to improve the GMB and ELA simulation, which requires further intensive observation and parameterization studies. The influence of snow redistribution on GMB and ELA are also worthwhile to be further investigated, as discussed in Section 5.3. Moreover, the FLEX^{G} model is at a daily time-step, but diurnal energy input variations or the effect of topographic shading may also impact

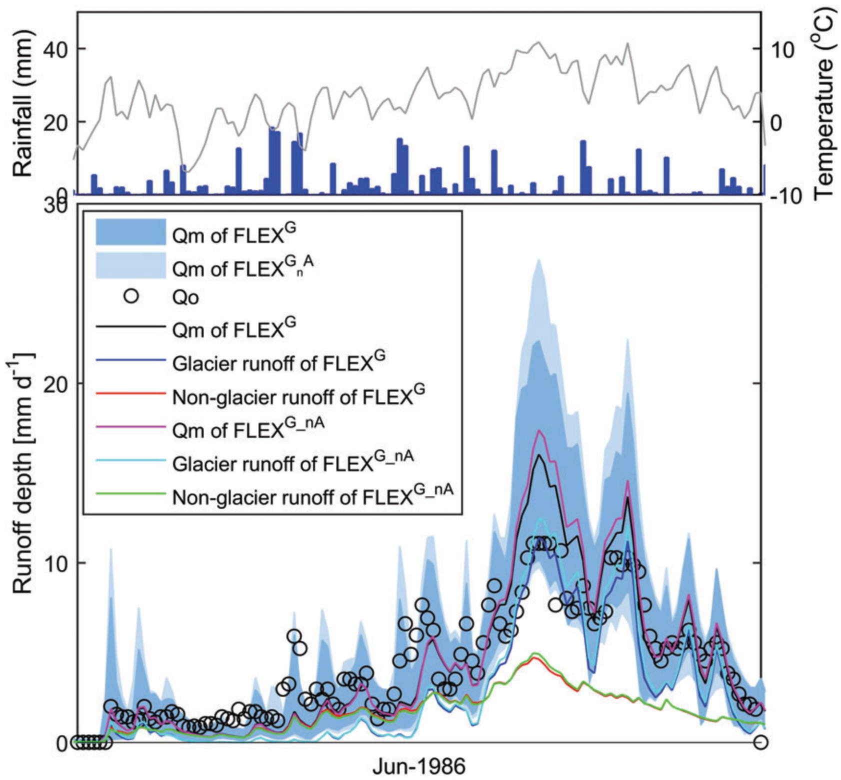

FIGURE 12 The model transferability results of FLEX^G and FLEX^{G_nA}. The observed hydrograph of the Zong Kong catchment is shown as black circles, and the uncertainty boundaries of the simulated hydrographs are shown in dark blue (FLEX^G) and light blue (FLEX^{G_nA}). The glacier runoff (blue line for FLEX^G and magenta line for FLEX^{G_nA}) and nonglacier runoff (red line for FLEX^G and green line for FLEX^{G_nA}) of two models are also shown, respectively

on snow and ice melting and thus the hydrologic response, which is worthwhile to further investigate with long-term and finer temporal resolution data.

A further limitation in the development of FLEX^G was the lack of stream flow observations after the end of the annual melt periods, that is, from September onwards. Model parameters associated with low-flow conditions, such as the groundwater recession parameter K_s, therefore remained hard to be identified. In addition, it is likely that river ice may also considerably influence and bias observations in spring and early summer.

6 | CONCLUSION

In this study, a semidistributed conceptual stream flow/glacier model was developed and tested against long-term glacier observations in a highly glaciered catchment, the Urumqi glacier no. 1 catchment (52% covered by glacier) in Central Asia. The main findings of this study can be summarized as

1. By including landscape characteristics, such as elevation, aspect distributions, and proportion of glacier cover, the FLEX^G model, calibrated for a small, highly glaciered headwater catchment could be robustly transferred and up-scaled to a larger catchment without the need for recalibration, indicating the value of including landscape heterogeneity in conceptual hydrological models.
2. The suggested FLEX^G model structure with temperature-index representations of snow and ice can, when adequately accounting for landscape-induced process heterogeneity, simultaneously satisfy more vigorous multiobjectives validation, such as reproduce the general variation of both hydrograph and snow pack as well as indicators for glacier variations, such as the annual GMB and the annual ELA.

ACKNOWLEDGMENTS

This work was supported by National Basic Research Program of China (2013CBA01808-A), State Key Laboratory of Cryospheric Sciences, Cold and Arid Regions Environment and Engineering Research Institute, Chinese Academy Sciences (SKLCS-OP-2016-04), and Natural Science Foundation of China (41130638, 41471001, 91547202, 51479216, and 41271090). The first author would like to thank professor Baisheng Ye, who generously shared data and made great contribution to this work. May he rest in peace. The authors are also grateful to the constructive discussions and suggestions from Daqing Yang, Jan Seibert, Shiqiang Zhang, and Xin Gao. Particularly, we would like to thank Wouter R. Berghuijs, Lei Wang, and other 3 anonymous reviewers for their extremely valuable and constructive comments and suggestions, which helped us to improve the paper.

REFERENCES

Anderton, S. P., White, S. M., & Alvera, B. (2004). Evaluation of spatial variability in snow water equivalent for a high mountain catchment. *Hydrological Processes*, *18*(3), 435–453. https://doi.org/10.1002/hyp.1319.

Andréassian, V., Le Moine, N., Perrin, C., Ramos, M.-H., Oudin, L., Mathevet, T., … Berthet, L. (2012). All that glitters is not gold: The case of calibrating hydrological models. *Hydrological Processes*, *26*, 2206–2210. https://doi.org/10.1002/hyp.9264.

Barry, R. G. (1992). *Mountain weather and climate*Psychology Press.

Berghuijs, W. R., Woods, R. A., & Hrachowitz, M. (2014). A precipitation shift from snow towards rain leads to a decrease in streamflow. *Nature Climate Change*, *4*, 583–586.

Berghuijs, W. R., Woods, R. A., Hutton, C. J., & Sivapalan, M. (2016). Dominant flood generating mechanisms across the United States. *Geophysical Research Letters*, *43*(9), 4382–4390. https://doi.org/10.1002/2016GL068070.

Beven, K., & Binley, A. (1992). The future of distributed models: Model calibration and uncertainty prediction. *Hydrological Processes*, *6*, 279–298. https://doi.org/10.1002/hyp.3360060305.

Beven, K., & Westerberg, I. (2011). On red herrings and real herrings: Disinformation and information in hydrological inference. *Hydrological Processes*, *25*, 1676–1680. https://doi.org/10.1002/hyp.7963.

Bhutiyani, M. R., Kale, V. S., & Pawar, N. J. (2008). Changing streamflow patterns in the rivers of northwestern Himalaya: Implications of global warming in the 20th century. *Curr. Sci. India.*, *95*(5), 618–626.

Biederman, J. A., Brooks, P. D., Harpold, A. A., Gochis, D. J., Gutmann, E., Reed, D. E., … Ewers, B. E. (2014). Multiscale observations of snow accumulation and peak snowpack following widespread, insect-induced lodgepole pine mortality. *Ecohydrology*, *7*(1), 150–162. https://doi.org/10.1002/eco.1342

Blöschl, G., Kirnbauer, R., & Gutknecht, D. (1991). Distributed snowmelt simulations in an alpine catchment: 1. Model evaluation on the basis of snow cover patterns. *Water Resources Research*, *27*, 3171–3179. https://doi.org/10.1029/91wr02250.

Braithwaite, R. J., & Olesen, O. B. (1989). In J. Oerlemans (Ed.), *Calculation of glacier ablation from air temperature, west greenland, glacier fluctuations and climatic change*. Dordrecht: Kluwer Academic Publisher.

Cheng, G., Li, X., Zhao, W., Xu, Z., Feng, Q., Xiao, S., & Xiao, H. (2014). *Integrated study of the water–ecosystem–economy in the heihe river basin, National Science Review*, https://doi.org/10.1093/nsr/nwu017.

Clark, M. P., Hendrikx, J., Slater, A. G., Kavetski, D., Anderson, B., Cullen, N. J., … Woods, R. A. (2011). Representing spatial variability of snow water equivalent in hydrologic and land-surface models: A review. *Water Resources Research*, *47*, W07539. https://doi.org/10.1029/2011wr010745.

Clark, M. P., Kavetski, D., & Fenicia, F. (2011). Pursuing the method of multiple working hypotheses for hydrological modeling. *Water Resources Research*, *47*, W09301. https://doi.org/10.1029/2010wr009827.

Cuffey, K. M., & Paterson, W. S. B. (2010). *The physics of glaciers* (fourth ed.). Burlington, USA: Elsevier.

Dadic, R., Mott, R., Lehning, M., & Burlando, P. (2010). Wind influence on snow depth distribution and accumulation over glaciers. *Journal of Geophysical Research: Earth Surface*, *115*(F1), n/a–n/a. https://doi.org/10.1029/2009JF001261.

Ding, Y., Liu, S., Li, J., & Shangguan, D. (2006). The retreat of glaciers in response to recent climate warming in western China. *Annals of Glaciology*, *43*, 97–105. https://doi.org/10.3189/172756406781812005.

Dong, Z., Qin, D., Ren, J., Li, K., & Li, Z. (2012). Variations in the equilibrium line altitude of Urumqi glacier no. 1, Tianshan Mountains, over the past 50 years. *Chinese Science Bulletin*, *57*, 4776–4783. https://doi.org/10.1007/s11434-012-5524-1.

Duethmann, D., Bolch, T., Farinotti, D., Kriegel, D., Vorogushyn, S., Merz, B., … Güntner, A. (2015). Attribution of streamflow trends in snow and glacier melt-dominated catchments of the Tarim River, Central Asia. *Water Resources Research*, *51*, 24.

Duethmann, D., Menz, C., Jiang, T., & Vorogushyn, S. (2016). Projections for headwater catchments of the Tarim River reveal glacier retreat and decreasing surface water availability but uncertainties are large. *Environmental Research Letters*, *11*, 054024.

Duethmann, D., Peters, J., Blume, T., Vorogushyn, S., & Güntner, A. (2014). The value of satellite-derived snow cover images for calibrating a hydrological model in snow-dominated catchments in Central Asia. *Water Resources Research*, *50*, 2002–2021.

Dunn, S. M., & Colohan, R. J. E. (1999). Developing the snow component of a distributed hydrological model: A step-wise approach based on multi-objective analysis. *Journal of Hydrology*, *223*, 1–16.

Euser, T., Hrachowitz, M., Winsemius, H. C., & Savenije, H. H. G. (2015). The effect of forcing and landscape distribution on performance and consistency of model structures. *Hydrological Processes*, *29*, 3727–3743. https://doi.org/10.1002/hyp.10445.

Euser, T., Winsemius, H. C., Hrachowitz, M., Fenicia, F., Uhlenbrook, S., & Savenije, H. H. G. (2013). A framework to assess the realism of model structures using hydrological signatures. *Hydrology and Earth System Sciences*, *17*(5), 1893–1912.

Fenicia, F., Kavetski, D., & Savenije, H. H. G. (2011). Elements of a flexible approach for conceptual hydrological modeling: 1. Motivation and theoretical development. *Water Resources Research*, *47*(11), n/a–n/a. https://doi.org/10.1029/2010WR010174.

Fenicia, F., Savenije, H. H. G., Matgen, P., & Pfister, L. (2008). Understanding catchment behavior through stepwise model concept improvement. *Water Resources Research*, *44*, W01402. https://doi.org/10.1029/2006wr005563.

Flowers, G. E., & Clarke, G. K. C. (2002). A multicomponent coupled model of glacier hydrology 2. Application to Trapridge Glacier, Yukon, Canada. *Journal of Geophysical Research: Solid Earth*, *107*, 2288. https://doi.org/10.1029/2001jb001124.

Freer, J. E., McMillan, H., McDonnell, J. J., & Beven, K. J. (2004). Constraining dynamic TOPMODEL responses for imprecise water table information using fuzzy rule based performance measures. *Journal of Hydrology*, *291*(3–4), 254–277. https://doi.org/10.1016/j.jhydrol.2003.12.037.

Fujihara, Y., Takase, K., Chono, S., Ichion, E., Ogura, A., & Tanaka, K. (2017). Influence of topography and forest characteristics on snow distributions in a forested catchment. *Journal of Hydrology*, *546*, 289–298. https://doi.org/10.1016/j.jhydrol.2017.01.021.

Fujita, K., & Sakai, A. (2014). Modelling runoff from a Himalayan debris-covered glacier. *Hydrology and Earth System Sciences*, *18*, 2679–2694. https://doi.org/10.5194/hess-18-2679-2014.

Fujita, K., Thompson, L. G., Ageta, Y., Yasunari, T., Kajikawa, Y., Sakai, A., & Takeuchi, N. (2006). Thirty-year history of glacier melting in the Nepal Himalayas. *Journal of Geophysical Research: Atmospheres*, *111*, D03109. https://doi.org/10.1029/2005jd005894.

Gao, H., He, X., Ye, B., & Pu, J. (2012). Modeling the runoff and glacier mass balance in a small watershed on the Central Tibetan Plateau, China, from 1955 to 2008. *Hydrological Processes*, *26*, 1593–1603. https://doi.org/10.1002/hyp.8256.

Gao, H., Hrachowitz, M., Fenicia, F., Gharari, S., & Savenije, H. H. G. (2014). Testing the realism of a topography-driven model (FLEX-Topo) in the nested catchments of the Upper Heihe, China. *Hydrology and Earth System Sciences*, *18*, 1895–1915. https://doi.org/10.5194/hess-18-1895-2014.

Gao, H., Hrachowitz, M., Schymanski, S. J., Fenicia, F., Sriwongsitanon, N., & Savenije, H. H. G. (2014). Climate controls how ecosystems size the root zone storage capacity at catchment scale. *Geophysical Research Letters*, *41*, 7916–7923. https://doi.org/10.1002/2014gl061668.

Garvelmann, J., Pohl, S., & Weiler, M. (2015). Spatio-temporal controls of snowmelt and runoff generation during rain-on-snow events in a mid-latitude mountain catchment. *Hydrological Processes*, *29*(17), 3649–3664. https://doi.org/10.1002/hyp.10460.

Gelfan, A. N., Pomeroy, J. W., & Kuchment, L. S. (2004). Modeling Forest cover influences on snow accumulation, sublimation, and melt. *Journal of Hydrometeorology*, *5*, 785–803. https://doi.org/10.1175/1525-7541(2004)005<0785:MFCIOS>2.0.CO;2.

Gharari, S., Hrachowitz, M., Fenicia, F., Gao, H., & Savenije, H. H. G. (2014). Using expert knowledge to increase realism in environmental system models can dramatically reduce the need for calibration. *Hydrology and Earth System Sciences*, *18*, 4839–4859. https://doi.org/10.5194/hess-18-4839-2014.

Goodison, B., Louie, P., & Yang, D. (1997). The WMO solid precipitation measurement intercomparison. *World Meteorological Organization-Publications-WMO TD, 65-70*.

Gupta, H. V., Kling, H., Yilmaz, K. K., & Martinez, G. F. (2009). Decomposition of the mean squared error and NSE performance criteria: Implications for improving hydrological modelling. *Journal of Hydrology*, *377*, 80–91. https://doi.org/10.1016/j.jhydrol.2009.08.003.

Gupta, H. V., Wagener, T., & Liu, Y. (2008). Reconciling theory with observations: Elements of a diagnostic approach to model evaluation. *Hydrological Processes*, *22*, 3802–3813. https://doi.org/10.1002/hyp.6989.

Hamon, W. R. (1961). Estimating potential evapotranspiration, Journal of the hydraulics division. *ASCE*, *87*, 107–120.

Han, C., Chen, R. S., Liu, J., Yang, Y., & Wenwu, Q. (2010). A discuss of separating solid and liquid precipitation. *Journal of Glaciology and Geocryology*, *32*, 249–256 (in Chinese).

He, Z. H., Tian, F. Q., Gupta, H. V., Hu, H. C., & Hu, H. P. (2014). Diagnostic calibration of a hydrological model in an alpine area by hydrograph partitioning. *Hydrology and Earth System Sciences Discussions*, *11*, 13385–13441. https://doi.org/10.5194/hessd-11-13385-2014.

Hock, R. (1999). A distributed temperature-index ice-and snowmelt model including potential direct solar radiation. *Journal of Glaciology*, *45*(149), 101–111.

Hock, R. (2003). Temperature index melt modelling in mountain areas. *Journal of Hydrology*, *282*, 104–115. https://doi.org/10.1016/S0022-1694(03)00257-9.

Hock, R. (2005). Glacier melt: A review of processes and their modelling. *Progress in Physical Geography*, *29*, 362–391. https://doi.org/10.1191/0309133305pp453ra.

Hrachowitz, M., Fovet, O., Ruiz, L., Euser, T., Gharari, S., Nijzink, R., … Gascuel-Odoux, C. (2014). Process consistency in models: The importance of system signatures, expert knowledge, and process complexity. *Water Resources Research*, *50*, 7445–7469. https://doi.org/10.1002/2014wr015484.

Hrachowitz, M., Savenije, H. H. G., Blöschl, G., McDonnell, J. J., Sivapalan, M., Pomeroy, J. W., … Cudennec, C. (2013). A decade of predictions in ungauged basins (pub)—A review. *Hydrological Sciences Journal*, *58*, 1198–1255. https://doi.org/10.1080/02626667.2013.803183.

Hrachowitz, M., & Weiler, M. (2011). Uncertainty of precipitation estimates caused by sparse gauging networks in a small, mountainous watershed. *Journal of Hydrologic Enginerring*, *16*, 460–471. https://doi.org/10.1061/(ASCE)HE.1943-5584.0000331.

Huang, J., Fu, Q., Zhang, W., Wang, X., Zhang, R., Ye, H., & Warren, S. G. (2010). Dust and black carbon in seasonal snow across northern China. *Bulletin of the American Meteorological Society*, *92*(2), 175–181. https://doi.org/10.1175/2010BAMS3064.1.

Huss, M., Jouvet, G., Farinotti, D., & Bauder, A. (2010). Future high-mountain hydrology: A new parameterization of glacier retreat. *Hydrology and Earth System Sciences*, *14*, 815–829. https://doi.org/10.5194/hess-14-815-2010.

Immerzeel, W. W., van Beek, L. P. H., & Bierkens, M. F. P. (2010). Climate change will affect the asian water towers. *Science*, *328*, 1382–1385. https://doi.org/10.1126/science.1183188.

Immerzeel, W. W., van Beek, L. P. H., Konz, M., Shrestha, A. B., & Bierkens, M. F. P. (2012). Hydrological response to climate change in a glacierized catchment in the Himalayas. *Climatic Change*, *110*(3), 721–736. https://doi.org/10.1007/s10584-011-0143-4.

Kienzle, S. W. (2008). A new temperature based method to separate rain and snow. *Hydrological Processes*, *22*(26), 5067–5085. https://doi.org/10.1002/hyp.7131.

Klemeš, V. 1990 The modelling of mountain hydrology: The ultimate challenge, IAHS report, Strbske Pleso, Czechoslovakia.

Konz, M., & Seibert, J. (2010). On the value of glacier mass balances for hydrological model calibration. *Journal of Hydrology*, *385*, 238–246. https://doi.org/10.1016/j.jhydrol.2010.02.025.

Konz, M., Uhlenbrook, S., Braun, L., Shrestha, A., & Demuth, S. (2007). Implementation of a process-based catchment model in a poorly gauged, highly glacierized himalayan headwater. *Hydrology and Earth System Sciences*, *11*, 1323–1339. https://doi.org/10.5194/hess-11-1323-2007.

Lanzhou Iinstitute of Glaciology and Geocryology, (2001). CAS, *Tianshan Glaciological Station Annual Report of Tianshan Glaciological Station*.

Li, X., Cheng, G., Liu, S., Xiao, Q., Ma, M., Jin, R., … Xu, Z. (2013). Heihe watershed allied telemetry experimental research (hiWATER): Scientific objectives and experimental design. *Bulletin of the American Meteorological Society*, *94*, 1145–1160. https://doi.org/10.1175/bams-d-12-00154.1.

Li, X., Wang, L., Chen, D., Yang, K., Xue, B., & Sun, L. (2013). Near-surface air temperature lapse rates in the mainland China during 1962–2011. *Journal of Geophysical Research: Atmospheres*, *118*, 7505–7515. https://doi.org/10.1002/jgrd.50553.

Li, Z., Wang, W., Zhang, M., Wang, F., & Li, H. (2010). Observed changes in streamflow at the headwaters of the Urumqi River, eastern Tianshan, Central Asia. *Hydrological Processes*, *24*, 217–224. https://doi.org/10.1002/hyp.7431.

Liu, S., Shangguan, D., Xu, J., Wang, X., Yao, X., Jiang, Z., … Wu, L. (2014). Glacier in china and their variations. In J. S. Kargel, G. J. Leonard, M. P. Bishop, A. Kääb, B. H. Raup, & H. Springer (Eds.), *Global land ice measurements from space* (pp. 583–608).

Martinec, J., Rango, A., Roberts, R., Baumgartner, M. F., & Apfl, G. M. (1998). *Snowmelt runoff model (SRM) user's manual*. Department of Geography: University of Berne.

Ming, J., Xiao, C., Du, Z., & Yang, X. (2013). An overview of black carbon deposition in high Asia glaciers and its impacts on radiation balance. *Advances in Water Resources*, *55*, 80–87. https://doi.org/10.1016/j.advwatres.2012.05.015.

Moore, R. D., Fleming, S. W., Menounos, B., Wheate, R., Fountain, A., Stahl, K., … Jakob, M. (2009). Glacier change in western North America: Influences on hydrology, geomorphic hazards and water quality. *Hydrological Processes*, *23*, 42–61. https://doi.org/10.1002/hyp.7162.

Oerlemans, J., & Fortuin, J. P. F. (1992). Sensitivity of glaciers and small ice caps to greenhouse warming. *Science*, *258*, 115–117. https://doi.org/10.1126/science.258.5079.115.

Ohmura, A., Konzelmann, T., Rotach, M., Forrer, J., Wild, M., Abe-Ouchi, A., and Toritani, H.: Energy balance for the greenland ice sheet by observation and model computation, snow and ice covers: Interactions with the atmosphere and ecosystems, Yokohama, 1994, 163–174.

Oudin, L., Michel, C., & Anctil, F. (2005). Which potential evapotranspiration input for a lumped rainfall-runoff model? Part 1—Can rainfall-runoff models effectively handle detailed potential evapotranspiration inputs? *Journal of Hydrology*, *303*(1–4), 275–289. https://doi.org/10.1016/j.jhydrol.2004.08.025.

Parajka, J., & Blöschl, G. (2008). The value of MODIS snow cover data in validating and calibrating conceptual hydrologic models. *Journal of Hydrology*, *358*, 240–258. https://doi.org/10.1016/j.jhydrol.2008.06.006.

Pohl, S., Garvelmann, J., Wawerla, J., & Weiler, M. (2014). Potential of a low-cost sensor network to understand the spatial and temporal dynamics of a mountain snow cover. *Water Resources Research*, *50*(3), 2533–2550. https://doi.org/10.1002/2013WR014594.

Pomeroy, J. W., & Essery, R. L. H. (1999). Turbulent fluxes during blowing snow: Field tests of model sublimation predictions. *Hydrological Processes*, *13*(August), 2963–2975. https://doi.org/10.1002/(SICI)1099-1085(19991230)13:18<2963::AID-HYP11>3.0.CO;2-9.

Pomeroy, J. W., Gray, D. M., Brown, T., Hedstrom, N. R., Quinton, W. L., Granger, R. J., & Carey, S. K. (2007). The cold regions hydrological model: A platform for basing process representation and model structure on physical evidence. *Hydrological Processes*, *21*, 2650–2667. https://doi.org/10.1002/hyp.6787.

Qin, D., & Ding, Y. (2010). Key issues on cryospheric changes, trends and their impacts. *Advances in Climate Change Research*, *1*, 1–10.

Raina, V. K., Srivastava, D., Singh, R. K., & Sangewar, C. V. (2008). Glacier regimen, fluctuation, hydrometry and mass transfer studies in the Himalayas. In V. K. Raina, & D. Srivastava (Eds.), *Glacier atlas of India* (pp. 206–216). Bangalore: Geol. Soc. India.

Refsgaard, J. C., Madsen, H., Andréassian, V., Arnbjerg-Nielsen, K., Davidson, T. A., Drews, M., … Christensen, J. H. (2014). A framework for testing the ability of models to project climate change and its impacts. *Climatic Change*, *122*, 271–282. https://doi.org/10.1007/s10584-013-0990-2.

Savenije, H. H. G. (2010). Hess opinions "topography driven conceptual modelling (FLEX-Topo)". *Hydrology and Earth System Sciences*, *14*, 2681–2692. https://doi.org/10.5194/hess-14-2681-2010.

Savenije, H. H. G., & Hrachowitz, M. (2017). HESS opinions "catchments as meta-organisms—A new blueprint for hydrological modelling". *Hydrology and Earth System Sciences*, *21*(2), 1107–1116. https://doi.org/10.5194/hess-21-1107-2017

Schaefli, B., Hingray, B., Niggli, M., & Musy, A. (2005). A conceptual glacio-hydrological model for high mountainous catchments. *Hydrology and Earth System Sciences Discussions*, *2*, 73–117. https://doi.org/10.5194/hessd-2-73-2005.

Schirmer, M., Wirz, V., Clifton, a., & Lehning, M. (2011). Persistence in intra-annual snow depth distribution: 1. Measurements and topographic control. *Water Resources Research*, *47*(9), n/a–n/a. https://doi.org/10.1029/2010WR009426.

Seibert, J. (1997). Estimation of parameter uncertainty in the HBV model. *Nordic Hydrology*, *28*, 247–262.

Seibert, J., Jenicek, M., Huss, M., & Ewen, T. (2015). Snow and ice in the hydrosphere. In W. Haeberli & C. Whiteman (Eds.), *Snow and ice-related hazards, risks, and disasters* (pp 99–130). Amsterdam: Elsevier.

Seibert, J., & McDonnell, J. J. (2002). On the dialog between experimentalist and modeler in catchment hydrology: Use of soft data for multicriteria model calibration. *Water Resources Research*, *38*(23), 1–14. https://doi.org/10.1029/2001WR000978.

Semenova, O., & Beven, K. (2015). Barriers to progress in distributed hydrological modelling. *Hydrological Processes*, *29*, 2074–2078. https://doi.org/10.1002/hyp.10434.

Shafii, M., Tolson, B., & Shawn, M. L. (2015). Addressing subjective decision-making inherent in GLUE-based multi-criteria rainfall–runoff model calibration. *Journal of Hydrology*, *523*, 693–705. https://doi.org/10.1016/j.jhydrol.2015.01.051.

Shi, Y., Huang, M., & Yao, T. (2000). *Glaciers and their environments in China—The present, past and future*. Beijing: Scienc Press.

Singh, P., Haritashya, U. K., & Kumar, N. (2008). Modelling and estimation of different components of streamflow for Gangotri Glacier basin, Himalayas. *Hydrological Sciences Journal*, *53*, 309–322. https://doi.org/10.1623/hysj.53.2.309.

Singh, P., Kumar, N., & Arora, M. (2000). Degree-day factors for snow and ice for Dokriani glacier, Garhwal Himalayas. *Journal of Hydrology*, *235*, 1–11.

Singh, P., & Singh, V. P. (2001). *Snow and glacier hydrology*. Dordrecht, the Netherlands: Kluwer Academic Publishers.

Sorg, A., Bolch, T., Stoffel, M., Solomina, O., & Beniston, M. (2012). Climate change impacts on glaciers and runoff in Tien Shan (Central Asia). *Nature Climate Change*, *2*, 725–731.

Sorg, A., Huss, M., Rohrer, M., & Stoffel, M. (2014). The days of plenty might soon be over in glacierized central Asian catchments. *Environmental Research Letters*, *9*, 104018.

Stahl, K., Moore, R. D., Floyer, J. A., Asplin, M. G., & McKendry, I. G. (2006). Comparison of approaches for spatial interpolation of daily air temperature in a large region with complex topography and highly variable station density. *Agricultural and Forest Meteorology*, *139*, 224–236. https://doi.org/10.1016/j.agrformet.2006.07.004.

Stahl, K., Moore, R. D., Shea, J. M., Hutchinson, D., & Cannon, A. J. (2008). Coupled modelling of glacier and streamflow response to future climate scenarios. *Water Resources Research*, *44*, W02422. https://doi.org/10.1029/2007wr005956.

Sun, B., He, M., Zhang, P., Jiao, K., Wen, J., & Li, Y. (2003). Determination of ice thickness, subice topography and ice volume at glacier no.1 in the Tien Shan, China, by ground penetrating radar. *Chinese Journal of Polar Research*, *15*, 35–44.

Thayyen, R. J., & Gergan, J. T. (2010). Role of glaciers in watershed hydrology: A preliminary study of a 'Himalayan catchment'. *The Cryosphere*, *4*(1), 115–128. https://doi.org/10.5194/tc-4-115-2010.

Thayyen, R. J., Gergan, J. T., & Dobhal, D. P. (2005). Monsoonal control on glacier discharge and hydrograph characteristics, a case study of Dokriani glacier, Garhwal Himalaya, India. *Journal of Hydrology*, *306*(1–4), 37–49.

Uhlenbrook, S., Roser, S., & Tilch, N. (2004). Hydrological process representation at the meso-scale: The potential of a distributed, conceptual catchment model. *Journal of Hydrology*, *291*, 278–296. https://doi.org/10.1016/j.jhydrol.2003.12.038.

Unger-Shayesteh, K., Vorogushyn, S., Farinotti, D., Gafurov, A., Duethmann, D., Mandychev, A., & Merz, B. (2013). What do we know about past changes in the water cycle of central Asian headwaters? *A review Glob. Planet. Change*, *110*, 4–25.

Wang, J., Ye, B., Cui, Y., He, X., & Yang, G. (2014). Spatial and temporal variations of albedo on nine glaciers in western China from 2000 to 2011. *Hydrological Processes*, *28*(9), 3454–3465. https://doi.org/10.1002/hyp.9883.

Wen, L., Nagabhatla, N., Lü, S., & Wang, S.-Y. (2013). Impact of rain snow threshold temperature on snow depth simulation in land surface and regional atmospheric models. *Advances in Atmospheric Sciences*, *30*(5), 1449–1460. https://doi.org/10.1007/s00376-012-2192-7.

Winstral, A., & Marks, D. (2002). Simulating wind fields and snow redistribution using terrain based parameters to model snow accumulation and melt over a semi-arid mountain catchment, Hydrol. *PRO*, *16*, 3585–3603.

Xie, Z., & Ge, G. (1965). Study of accumulation, ablation and mass balance of glacier no. 1 at the headwater of Urumqi River, tianshan. In *Study of glaciology and hydrology on the Urumqi River, Tianshan* (pp. 14–24). Beijing: Science Press.

Yang, D., Goodison, B., Metcalfe, J., Louie, P., Elomaa, E., Hanson, C., … Lapin, M. (2001). Compatibility evaluation of national precipitation gage measurements. *Journal of Geophysical Research*, *106*, 1481–1491. https://doi.org/10.1029/2000jd900612.

Yang, D., Jiang, T., Zhang, Y., & Kang, E. (1988). Analysis and correction of errors in precipitation measurement at the head of Urumqi River, Tianshan. *Journal of Glaciology and Geocryology*, *10*, 384–400.

Yang, M., Ye, B., Peng, P., Han, T., Gao, H., Cui, Y., … Gao, M. (2012). HBV model glacier runoff degree-day factor glacier area change glacier volume change. *Journal of Glaciology and Geocryology*, *34*, 130–138.

Yang, D., Zhang, Y., & Zhang, Z. (1992). A study on the snow density in the head area of Urumqi River basin. *Acta Geographica Sinica*, *47*, 260–266.

Yao, T., Pu, J., Lu, A., Wang, Y., & Yu, W. (2007). Recent glacial retreat and its impact on hydrological processes on the Tibetan Plateau, China, and surrounding regions. *Arctic, Antarctic, and Alpine Research*, *39*, 642–650. https://doi.org/10.1657/1523-0430(07-510)[yao]2.0.co;2.

Yao, T., Thompson, L., Yang, W., Yu, W., Gao, Y., Guo, X., … Joswiak, D. (2012). Different glacier status with atmospheric circulations in Tibetan Plateau and surroundings. *Nature Clim. Change*, *2*, 663–667. https://doi.org/10.1038/NCLIMATE1580.

Ye, B., Yang, D., Jiao, K., Han, T., Jin, Z., Yang, H., & Li, Z. (2005). The Urumqi River source glacier no. 1, Tianshan, China: Changes over the past 45 years. *Geophysical Research Letters*, *32*, L21504. https://doi.org/10.1029/2005gl024178.

Zhang, J. (1981). Mass balance studies on glacier no. 1 in Urumqi River, Tianshan. *Journal of Glaciology and Geocryology*, 32–40.

Zhang, J., Li, Q., Guo, B., & Gong, H. (2015). The comparative study of multi-site uncertainty evaluation method based on SWAT model. *Hydrological Processes*, *29*(13), 2994–3009.

Zhang, Y., Liu, S., & Ding, Y. (2006). Observed degree-day factors and their spatial variation on glaciers in western china. *Annals of Glaciology*, *43*, 301–306. https://doi.org/10.3189/172756406781811952.

Zhao, W., & Cheng, G. (2002). Review of several problems on the study of eco-hydrological processes in arid zones. *Chinese Science Bulletin*, *47*, 353–360. https://doi.org/10.1360/02tb9084.

Zhao, R.-J., & Liu, X. R. (1995). The Xinangjiang model. In V. P. Singh (Ed.), *Computer models of watershed hydrology* (pp. 215–232).

Zhao, Q., Ye, B., Ding, Y., Zhang, S., Yi, S., Wang, J., … Han, H. (2013). Coupling a glacier melt model to the variable infiltration capacity (VIC) model for hydrological modeling in north-western China. *Environment and Earth Science*, *68*, 87–101. https://doi.org/10.1007/s12665-012-1718-8.

Zhou, H.-F., Zheng, X.-J., Zhou, B., Dai, Q., & Li, Y. (2012). Sublimation over seasonal snowpack at the southeastern edge of a desert in central Eurasia. *Hydrological Processes*, *26*(25), 3911–3920. https://doi.org/10.1002/hyp.8402.

SUPPORTING INFORMATION

Additional Supporting Information may be found online in the supporting information tab for this article.

How to cite this article: Gao H, Ding Y, Zhao Q, Hrachowitz M, Savenije HHG. The importance of aspect for modelling the hydrological response in a glacier catchment in Central Asia. *Hydrological Processes*. 2017;31:2842–2859. https://doi.org/10.1002/hyp.11224